Application of frequency ratio model and GIS on susceptibility mapping of ground subsidence influenced by earthquake

Taeyoo Na

A Thesis in the Department of Geosciences, Geotechnology and Material Engineering for Resources and the Faculty of Graduate School of International Resource Sciences for the Degree of Doctor of Resource Science

Akita University

September 2021

Abstract

Land subsidence is one of typical secondary disaster related to earthquake and occurs annually, worldwide. Accordingly, large economic losses and deaths in densely industrialized and highly populated urban areas as a result of these hazards. As a major earthquake occurred in Iburi subprefecture, Japan on September 2018, Sapporo has also damaged by ground subsidence.

The purpose of this study is assessing the vulnerability of earthquake-induced land subsidence in Sapporo, Japan and produce susceptibility map. For this aim, bivariate statistical analysis method (frequency ratio model) and geographic information system (GIS) technique were applicated. For the susceptibility modelling, past ground subsidence location map was prepared. And seven ground subsidence causative factors were considered for the subsidence probability analysis include: geology, slope angle, land use, ground water level, distance from railroad and subway line, intensity of earthquake (MMI) and rainfall. Weightage for each conditioning factors were identified using frequency ratio model to assess subsidence susceptibility index and mapped using GIS.

Area under curve (AUC) was applied to verify the performance of predicted model using prepared past ground subsidence location map. The prediction accuracies were (1) 85.17% for Higashi ward, (2) 95.44% for Kiyota ward and (3) 83.22 for Sapporo, respectively.

This result showed sufficient possibility for reliable susceptibility mapping of ground subsidence using GIS and frequency ratio model. EGSSM can be used as a helpful material on ground subsidence risk influenced by earthquake to reduce the scale of damages and manage in advance, effectively. The result of this study can be used as a helpful material for the disaster risk mitigation and efficient management in urban area.

Keywords: Ground subsidence, Earthquake, Ground subsidence susceptibility, Frequency ratio model, GIS.

Acknowledgments

First of all, I would like to thank to Prof. Youhei Kawamura for his kind advices and supervision for my research from my first semester as a doctoral student to graduation. Also, feel deep gratitude for his supports and encouragements in every moment when I had many concerns and troubles.

And I would like to thank to Prof. Seong-seung Kang who was my advisor professor from bachelor to master student in Chosun University. Without his sincere advice and teaching, this special chance of studying at Akita University and valuable experiences would not have been possible.

I also appreciate to my dissertation examiner professors, Prof. Tsuyoshi Adachi, Prof. Daizo Ishiyama and Prof. Tadao Imai for their advices and comments.

Thank you to Ministry of Education, Culture, Sports, Science and Technology (MEXT) that give me the scholarship during three years of my doctoral student course in Akita University. Thanks to the financial support, I could focus to my research and get good results of that. And I would like thanks to International Resource Sciences Section of Academic Affairs Division and International Affairs Division of Akita University for their kind helps and supports for the university life, research and life in Japan.

I also thanks to Ms. Watanabe for her kindness and support in many of aspects during living in Japan from when I was firstly coming to Akita. Also, thank you to Prof. Jin-yeol Gong and his wife for inviting me and my wife to their house and serving delicious foods and letting us have a good time.

Thanks to Prof. Toriya, Dr. Dorjsuren, graduated guys: Yoshio, Jaewon, Donghyun, Yusang, Mingu, Jo, Natsuo, Jun, Yumi, Umeda, Rei, Rempei, Takeuchi and my lab members, Ph.D. students: Zed, Brian, Elsa, Kursat, Ikeda, master students: Jalali, Elisha, Senjoba, Daniyar, Taiga, Yoshino, Yuhei, Owada, Bat-erdene, Khangerel, bachelor students: Tatsuki, Takaya, Shinichiro, Tomoya.

Lastly, I am very appreciating to my father, Gwang-chul Na, my mother, Na-mi Kim, my father-in-law, Doo-seok Mun, my mother-in-law, Chun-rae Im, my older brother, Tae-woong Na for their devoted love and encouragement. Also, I specially thanks to my wife, Hee-suk Mun from bottom to my heart for her decision to come to Japan even quit her job for me. Also, truly thanks for her dedication, understanding and support. I would like to say that I have never forgotten the consideration, dedication and support I have received.

Taeyoo Na

Table of Contents

List of Tables

List of Figures

Chapter I

Introduction

1.1 Background

Now, ground subsidence occurs frequently worldwide and the damage from this risk is increasing. In big cities, as population growth and man-made structures are increasing more and more, huge scale of damage on human lives and economic aspect have been occurred by ground subsidence. In urban areas, ground subsidence can be occurred by results of human activities such as construction of underground structures and groundwater extraction (Ezquerro et al. 2017; Kaitantzian et al. 2020). Also, soil liquefaction is well known as a major reason on ground subsidence occurrence (Avilés-Campoverde et al. 2021; Li et al. 2021). Regarding this, earthquake, one of the important natural hazards, is the trigger of this liquefaction phenomenon. In Japan, earthquakes have occurred on various scale, frequently and there have been more than 70 major earthquakes in the past current decades. On September 6, 2018, a strong earthquake has occurred in Iburi Subprefecture which is named as 2018 Hokkaido Eastern Iburi earthquake. Magnitude of this earthquake was 6.6 M_W and maximum MMI was 12. This earthquake resulting a lot of casualties, injuries and severe economic losses. And most of damage was caused by landslides and ground subsidence those affected by earthquake. The study area of Sapporo has also damaged by ground subsidence due to this earthquake and occurred widely in two wards of Higashi and Kiyota.

Normally, restoration work has been carried out as a countermeasure after the damage but it costs high and also having difficulties on complete restore, especially in urban areas. For this reason, predict and measure the earthquake-induced ground subsidence is very important for the reduction of disaster hazards and management. A number of studies have conducted on assessment of ground subsidence in urban areas (Zhou et al. 2019; Blasco et al. 2019; Khorrami et al. 2020; Sevil et al. 2020; Maghsoudi et al. 2021). Also, several quantitative analysis models and GIS have been applied in previous studies for evaluating risk of ground subsidence. However, despite of many studies on ground subsidence have conducted, it has been not well studied concerning assessment of earthquake-induced ground subsidence in urban areas.

1.2 Research Aim and Objectives

The main purpose of current study is vulnerability assessment of earthquake-induced ground subsidence in urban area and produce hazard susceptibility map. For this purpose, Sapporo city, Hokkaido in Japan where subsidence has occurred by 2018 Hokkaido Eastern Iburi earthquake was selected as study area and ground subsidence location map was prepared. Also, seven subsidence causative factors were selected and considered to identify correlation between ground subsidence occurrence: geology, slope angel, land use, ground water level, distance from railroad and subway line, precipitation and intensity of earthquake (MMI). Frequency ratio (FR) model was applied that has previously demonstrated as having good performance on disaster risk prediction findings in previous researches for the quantitative subsidence probability analysis. From the

analysis results, ground subsidence susceptibility index (GSSI) was identified and earthquake-induced ground subsidence susceptibility map (EGSSM) was constructed in the geographic information system (GIS) environment. Area under the curve approach was applicated for the verification of prediction accuracy of the hazard map using prepared past ground subsidence location map. The objectives for the main aim of this study could be summarized as below:

- Collect and extract database of ground subsidence causative factors and actual ground subsidence area from reasonable agencies websites and geology company.
- Determine the relationship between ground subsidence and conditioning factors.
- Produce earthquake-induced ground subsidence susceptibility map (EGSSM) for the visualization.
- Examine the prediction accuracy of EGSSM by comparing data of actual ground subsidence area.

1.3 Outline of Dissertation

This dissertation is composed of total five chapters to provide understanding of vulnerability risk assessment and early warning of ground subsidence and earthquake using geospatial techniques, quantitative and probability analysis method. Chapter I presents background, main aim and objectives of this study. Chapter II introduce literatures review regarding ground subsidence and earthquake. Also including, ground subsidence susceptibility mapping and potential ground subsidence risk assessment methods. Chapter III provides information of three study areas, methodology, considered

seven ground subsidence conditioning factors, borehole database, applicated analysis and verification methods. Chapter IV presents results and discussion for each study areas. In chapter V, conclusion, limitation of this work and recommendation are provided for the future study.

Chapter II

Literature Review

2.1 Earthquake-induced ground subsidence

2.1.1 Ground subsidence

Ground subsidence (or land subsidence) is generally defined as a gradual settling to downward or sudden sinking of the ground's surface. Ground subsidence occurrence is not limited by the place and it can be occurred by natural processes like dissolution of limestone, earthquake, intensive rainfall, climate changes, groundwater-related subsidence and faulting. Also, can be caused by human activities; activity of mining (extraction of minerals and natural gas), extraction of ground water and construction of underground structures.

In urban environment, ground subsidence may be occurred by some typical reasons. Regarding human activities, excessive extraction of ground water (Holzer and Johnson, 1985) is one of the most well-known reason of ground subsidence in urban area. In the case of natural causes, ground subsidence occurrence has been considered as one of the most typical effects by the earthquake. From the past to present, earthquakes have occurred continuously and frequently world-wide, and as a result it caused severe damages in big cities by ground subsidence.

Damages by the ground subsidence in urban area can be occurred in several aspects including human lives, properties, houses and infrastructures, etc. Abidin et al.

(2015) classified the impacts of ground subsidence in big cities into aspect of infrastructure, environment, economy and society as shown in the Table 1.

Table 1. Categorized impacts of ground subsidence (Abidin et al. 2015).

No.	Category	Representation of impact	Level of impact
1	Infrastructural	cracking of permanent constructions and roads	Direct
		tilting of houses and buildings	Direct
		'sinking' of houses and buildings	Direct
		breaking of underground pipelines and utilities	Direct
		malfunction of sewerage and drainage system	Indirect
		deterioration in function of building and infrastructures	Indirect
2	Environmental	changes in river canal and drain flow systems	Indirect
		frequent coastal flooding	Indirect
		wider expansion of flooding areas	Indirect
		inundated areas and infrastructures	Indirect
		increased inland sea water intrusion	Indirect
		deterioration in quality of environmental condition	Indirect
3	Economic	increase in maintenance cost of infrastructure	Indirect
		decrease in land and property values	Indirect
		abandoned buildings and facilities	Indirect
		disruption to economic activities	Indirect
4	Social	deterioration in quality of living environment and life (e.g. health and sanitation condition)	Indirect
		disruption to daily activities of people	Indirect

2.1.2 Earthquake Events in the World

Earthquake is one of the most main causes of ground subsidence occurrence. Thus, it can be explained as there is a close correlation between earthquake and ground subsidence (Cotecchia, 1986). During the strong ground shaking by earthquake, ground subsidence can occur in various areas with diverse reasons. According to the United States Geological Survey (USGS), there were 1,518 earthquakes with magnitude over 6 have occurred worldwide in the past 10 years (Figure 1). And more than 150 earthquake events have stroke globally with magnitude over 7 in this period.

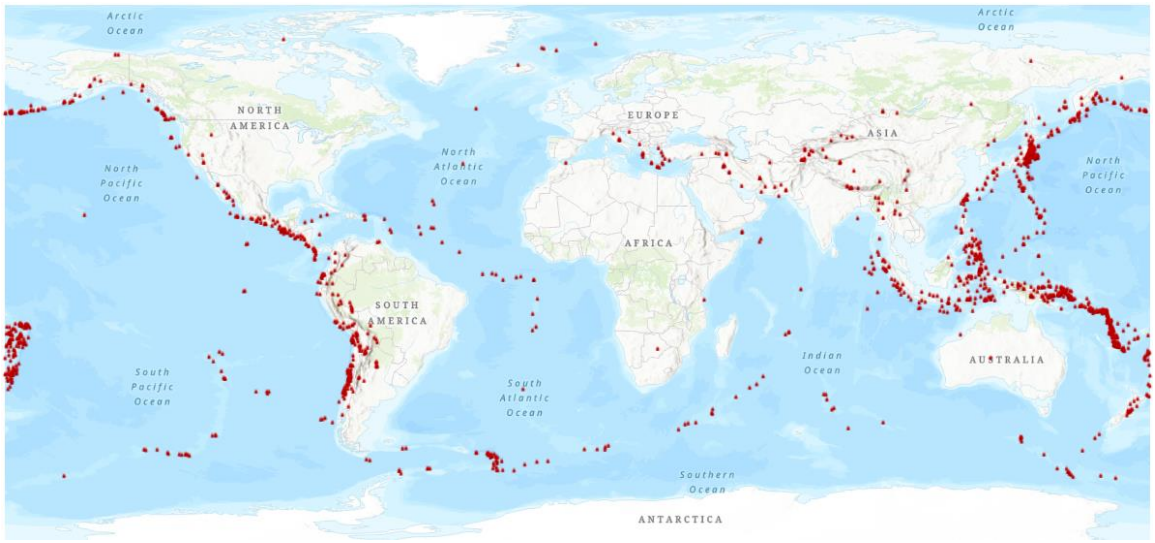

Figure 1. Earthquakes in past 10 years worldwide (USGS).

Since 20th century, there were 20 largest earthquake events in the world (Table 2). Minimum magnitude was recorded 8.4 which has occurred in Indonesia, Peru and Japan. And maximum magnitude was 9.5 earthquake that occurred in Chile, 1960. Result of earthquakes striking, there were massive casualties and economic losses worldwide.

Table 2. Twenty largest earthquakes in the world (USGS).

	Mag	Location	Alternative Name	Date (UTC)	Time (UTC)	Latitude	Longitude
1	9.5	Bio-Bio, Chile	Valdivia Earthquake	1960-05-22	19:11	38.14°S	73.41°W
2	9.2	Southern Alaska	1964 Great Alaska Earthquake, Prince William Sound Earthquake, Good Friday Earthquake	1964-03-28	03:36	60.91°N	147.34°W
3	9.1	Off the West Coast of Northern Sumatra	Sumatra-Andaman Islands Earthquake, 2004 Sumatra Earthquake and Tsunami, Indian Ocean Earthquake	2004-12-26	00:58	3.30°N	95.98°E
4	9.1	Near the East Coast of Honshu, Japan	Tohoku Earthquake	2011-03-11	05:46	38.30°N	142.37°E
5	9.0	Off the East Coast of the Kamchatka Peninsula, Russia	Kamchatka, Russia	1952-11-04	16:58	52.62°N	159.78°E
6	8.8	Offshore Bio-Bio, Chile	Maule Earthquake	2010-02-27	06:34	36.12°S	72.90°W
7	8.8	Near the Coast of Ecuador	1906 Ecuador–Colombia Earthquake	1906-01-31	15:36	0.96°N	79.37°W
8	8.7	Rat Islands, Aleutian Islands, Alaska	Rat Islands Earthquake	1965-02-04	05:01	51.25°N	178.72°E
9	8.6	Eastern Xizang-India border region	Assam, Tibet	1950-08-15	14:09	28.36°N	96.45°E
10	8.6	Off the West Coast of Northern Sumatra		2012-04-11	08:39	2.33°N	93.06°E

Table 2. (continued)

	Mag	Location	Alternative Name	Date (UTC)	Time (UTC)	Latitude	Longitude
11	8.6	Northern Sumatra, Indonesia	Nias Earthquake	2005-03-28	16:10	2.09°N	97.11°E
12	8.6	Andrean of Islands, Aleutian Islands, Alaska		1957-03-09	14:23	51.50°N	175.63°W
13	8.6	South of Alaska	Unimak Island Earthquake, Alaska	1946-04-01	12:29	53.49°N	162.83°W
14	8.5	Banda Sea		1938-02-01	19:04	5.05°S	131.61°E
15	8.5	Atacama, Chile	Chile-Argentina Border	1922-11-11	04:33	28.29°S	69.85°W
16	8.5	Kuril Islands		1963-10-13	05:18	44.87°N	149.48°E
17	8.4	Near the East Coast of Kamchatka Peninsula, Russia	Kamchatka, Russia	1923-02-03	16:02	54.49°N	160.47°E
18	8.4	Southern Sumatra, Indonesia		2007-09-12	11:10	4.44°S	101.37°E
19	8.4	Near the Coast of Southern Peru	Arequipa, Peru Earthquake	2001-06-23	20:33	16.27°S	73.64°W
20	8.4	Off the East Coast of Honshu, Japan	Sanriku, Japan	1933-03-02	17:31	39.21°N	144.59°E

For example, by the impacts of 1964 Prince William Sound Earthquake, Alaska, United States, there were 131 casualties. Moreover, it caused severe damage in many towns including building collapse, destruction of residential areas, occurrence of huge scale of landslides and vertical displacement. Estimated properties damage was about 2.3 billion dollars (USGS).

Due to frequent earthquakes in the world as mentioned above, the occurrence and damage of ground subsidence is also increasing. And according to scale of the earthquake, the scale and damage by the ground subsidence also increases dramatically to the aspects of human lives, properties, infrastructure, etc. Thus, it is crucial that considering the relation to earthquakes together in the evaluation of ground subsidence hazards.

2.1.3 Earthquake Events in Japan

Japan is already well known as one of the most earthquake-prone countries in the world. In Japan, more than 980 earthquake (MMI 6 or higher) including around 70 major earthquakes have occurred in past decade, nationwide. Among those earthquakes, 74 earthquakes with a MMI of more than eight were reported (Japan Meteorological Agency). Due to these frequent earthquakes, Japan suffers a lot of casualties and economic losses every year. As a representative event, massive earthquake (magnitude of 9) occurred on 11 March, 2011 at off the Pacific coast of the northeastern part of the Japanese main land. The earthquake named as 2011 Great East Japan Earthquake was the largest earthquake in Japan history. Because of the huge scale of tsunami caused by this earthquake, more than 15,000 people were dead and more than 2,900 people were

missing. Moreover, caused disastrous damages such as caused by ground subsidence and landslide occurrence in many cities around Kanto region and failure of nuclear power plant in Fukushima, etc. (Yasuda et al. 2012).

Hokkaido prefecture is secondly largest island of Japan and one of the most earthquake-prone regions. On September 6, 2018, Hokkaido Eastern Iburi earthquake has occurred in Iburi subprefecture (Epicenter: 42.691°N, 142.007°E, depth: 37.0 km, M 6.7). Figure 2 shows the location of epicenter and degree of seismic intensity (JMA) of 2018 Hokkaido Eastern Iburi Earthquake by regions.

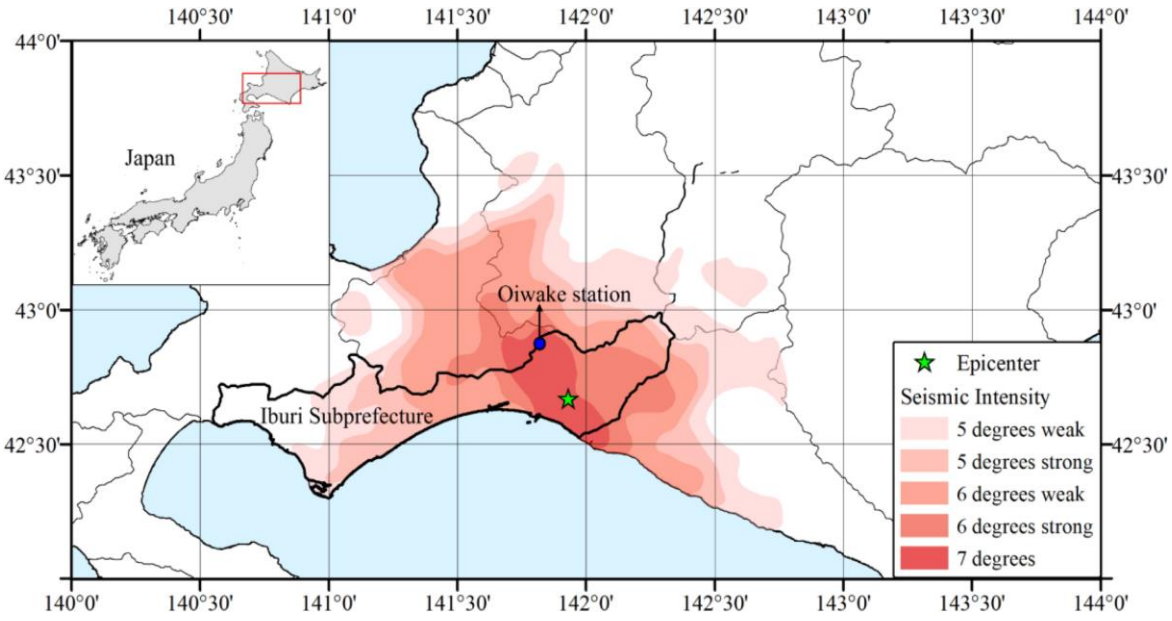

Figure 2. Epicenter location and Intensity of 2018 Hokkaido Eastern Iburi Earthquake (Zhou et al. 2021).

The earthquake caused 42 deaths and 762 people were injured. Moreover, it caused massive damage to social infrastructures such as houses, farmland, roads in a wide range of areas in Hokkaido. Estimated economic losses was around 114.5 billion yen (Japanese Geotechnical Society, 2019). Sapporo city, (capital city of Hokkaido Prefecture and Ishikari Prefecture) where located more than 50 kilometers from the epicenter, also damaged by ground subsidence occurrence.

2.2 Ground Subsidence Hazard Assessment Methods

Recently, many of studies have conducted by applicate various quantitative analysis models based on the geographic information system (GIS) to assess and predict the ground subsidence hazards and produce susceptibility map. GIS based researches have highly contributed on various hazards assessment with its efficient and advanced techniques in gathering data, analysis and also verification process (Pradhan et al. 2014).

So far, a number of researchers have conducted hazard mapping on ground subsidence using various quantitative analysis models with GIS techniques: evidential belief function model (Pradhan et al. 2014; Najafi et al. 2020), logistic regression model (Kim et al. 2006; Park et al. 2014;), weight of evidence model (Oh and Lee, 2010; Perrin et al. 2015), frequency ratio model (Choi et al. 2007 and Oh et al. 2011), support vector machine model (Abdollahi et al. 2019; Mohammady et al. 2019), fuzzy operator (Choi et al. 2010; Bianchini et al. 2019) and artificial neural network (ANN) (Kim et al. 2009 and Lee et al. 2012).

Pradhan et al. (2014) applicated multivariate statistical analysis method (evidential belief function model, EBF) and frequency ratio model for the estimation of

sinkhole type subsidence hazards at Kinta Valley of Perak, Malaysia. In this research, EBF model had better performance in subsidence hazard mapping. Kim et al. (2006) generated ground subsidence hazard map in around abandoned underground coal mines (AUCMs) at Samcheok City in Korea. Research had conducted by using and comparing two statistical approaches including logistic regression model and frequency ratio model. A developed method for evaluate the conditioning factors related to the sinkhole occurrence in a context of limestone karst using weight-of-evidence analysis was suggested by Perrin et al. (2015). Abdollahi et al. (2019) provided land subsidence susceptibility map in Kerman province, Iran using support vector machine (SVM) model. Five fuzzy operator was applicated to estimate the vulnerable areas to ground subsidence in Taebaek City, Korea and advantages of fuzzy combination operators were proposed by Choi et al. (2010). Kim et al. (2009) and Lee et al. (2012) applicated artificial neural network (ANN) and GIS to construct potential ground subsidence risk map in around abandoned underground coal mines in Korea.

In recent studies, researchers have conducted assessment of ground subsidence susceptibility by using and comparing several models for more accurate and reliable results. Bui et al. (2018) assessed subsidence susceptibility using four machine learning models including Bayesian Logistic Regression (BLR), Support Vector Machine (SVM), Logistic Model Tree (LMT) and Alternate Decision Tree (ADTree).

Mohammady et al. (2019) compared weight of evidence model and support vector machine model to assess subsidence susceptibility in Semnan plain, Iran. Rehman et al. (2020) analyzed mining subsidence susceptibility in Raniganj coalfield using frequency ratio, statistical index and Mamdani fuzzy models.

Probabilistic approaches including evidential belief function (EBF) and Bayesian theory (BT) have applied for the land subsidence susceptibility zonation (Najafi et al. 2020).

Some of study have conducted with ensembled two or more analysis methods to obtain higher prediction accuracy on subsidence susceptibility assessment. Arabameri et al. (2020) suggested ANN-bagging method for the land subsidence susceptibility mapping in Semnan Plain of Iran. They compared three different models include ANN, bagging and ANN-bagging and showed the most reliable prediction was obtained from ensembled ANN-bagging model.

Bayesian, functional, and meta-ensemble machine learning models were applied and compared to produce land subsidence susceptibility map in Hwajeon, Korea (Oh et al. 2019). Compared results showed meta-ensemble machine learning model had the highest prediction accuracy.

Ilia et al (2018) predicted land subsidence and identified spatiotemporal pattern of groundwater resources in Western Thessaly, Greece using remote sensing and random forest method. Some of study have conducted with ensembled two or more analysis methods to obtain higher prediction accuracy on subsidence susceptibility assessment.

Though, despite above numerous researches on ground subsidence have been undertaken, regarding the earthquake-induced ground subsidence in urban areas has not been studied. And as well as it has not been considered and analyzed about the correlation between ground subsidence occurrence and conditioning factors related with subsidence, under same situation above.

2.3 Earthquake-induced Subsidence Hazard Assessment in Hokkaido

In recent decade, as the major earthquake (named as 2018 Hokkaido Eastern Iburi Earthquake) event has occurred in Hokkaido, many of studies have conducted related with this disaster. About studies related with the topic of this thesis (hazard mapping for the assessment of ground subsidence that strongly influenced by earthquake in urban area), we found that most of studies performed related with assessment of earthquake-induced landslides (Aimaiti et al. 2019; Nam and Wang, 2019; Zhou et al. 2021). Nam and Wang (2019) assessed susceptibility of landslides that influenced by earthquake using autoencoder framework based on deep neural network and GIS (Figure 3).

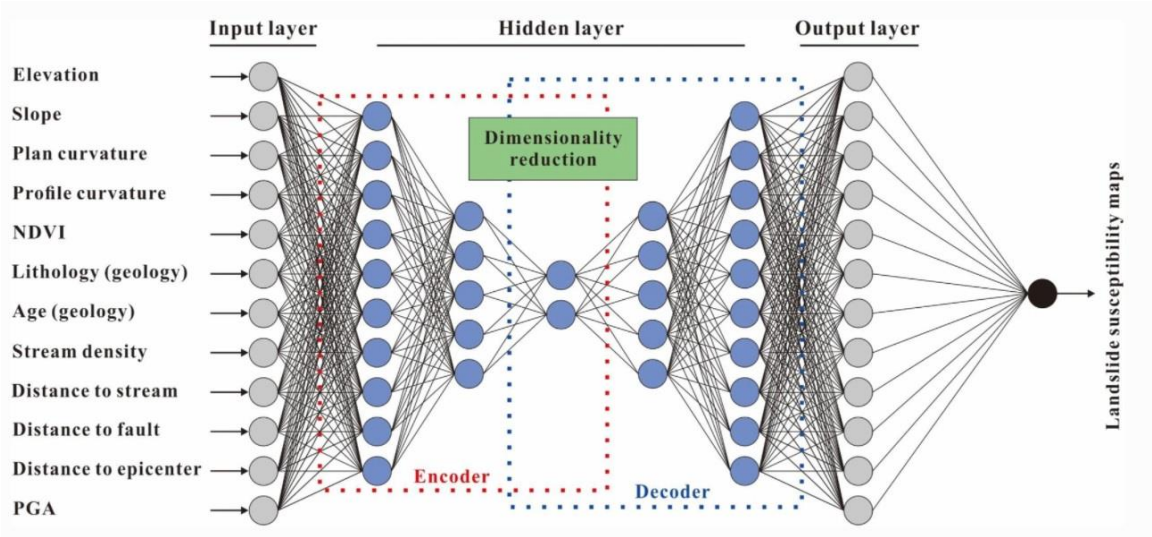

Figure 3. Architecture of autoencoder framework (Nam and Wang, 2019).

Some of the researchers identified and interpreted ground displacements and assess the damage by 2018 Hokkaido Eastern Iburi Earthquake. For the analysis, remote sensing techniques were applicated (Karimzadeh et al. 2018; Fujiwara et al. 2019). For an

instance, Karimzadeh et al. (2018) applicated interferometric synthetic aperture radar (InSAR) technique to detect the liquefaction-related damages and surface displacements in urban area. For the purpose, weighted overlay (WO) analysis performed with influential parameters including space-based InSAR results, ground-based LiquickMap and topographic slope (Figure 4).

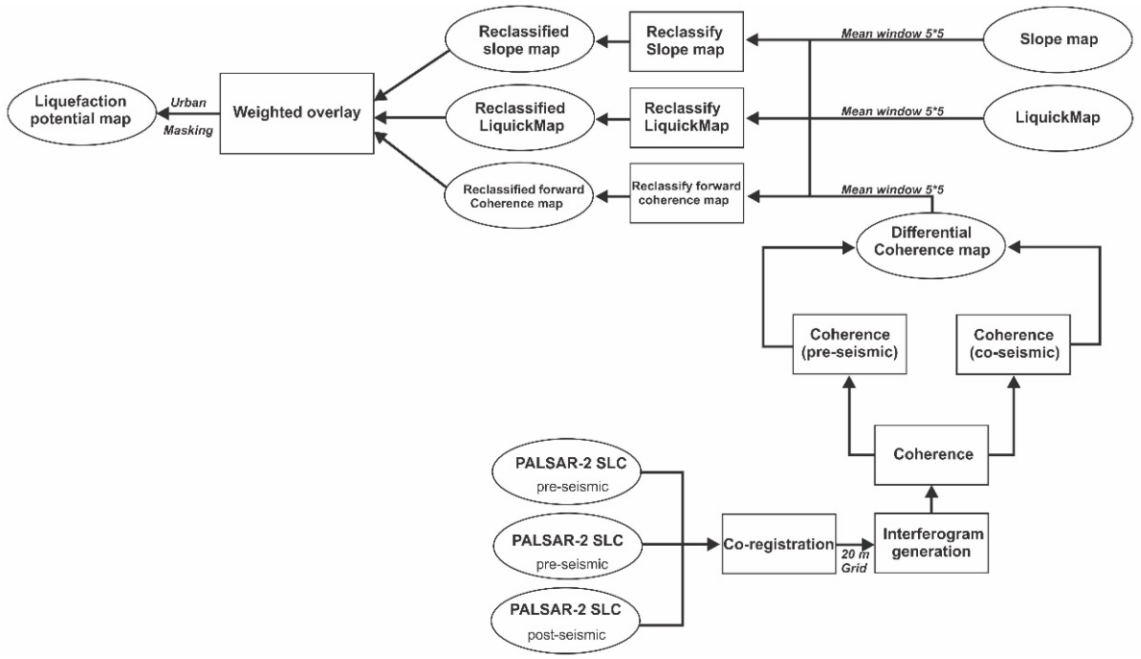

Figure 4. Weighted overlay (WO) analysis using synthetic aperture radar (SAR) coherence (Karimzadeh et al. 2018).

However, these studies were focused on the detection and observation of liquefaction and landslides. After literature review, confirmed that there was no research related with assessment of earthquake-induced ground subsidence hazard, especially in Sapporo and Hokkaido. Thus, ground subsidence caused by earthquake is a new subject.

Chapter III

Materials and Methods

3.1 Study Areas

3.1.1 Higashi-Ward of Sapporo

Study area, Higashi ward (East area) of Sapporo, is one of the 10 wards in Sapporo, Hokkaido, Japan. And Sapporo is capital city of Hokkaido Prefecture and its Ishikari Subprefecture. Study area is located in the southwest part of Ishikari Plain and the alluvial fan of the Toyohira River, a tributary stream of the Ishikari River. Higashi-Ward is lies between 43°4'8"N - 43°10'3"N and 141°20'35"E - 141°27'25"E. And total study area is 56.97 km2. Hokkaido is one of the most earthquake-prone areas in Japan and there have been 93 earthquakes which over 6 Modified Mercalli Intensity scale (MMI) in past decade (Meteorological agency of Japan). Accordingly, as one of damages from earthquake, there has always been danger of ground subsidence in this area. On September 6, 2018, great earthquake (2018 Hokkaido Eastern Iburi earthquake, Maximum MMI 12) occurred in Iburi Subprefecture, southern Hokkaido. Result of the earthquake, there were 42 confirmed deaths and 762 people were injured. Also, the earthquake caused serious damage of properties and total damage was estimated at around 114.5 billion yen (Japanese Geotechnical Society, 2019). Study area has also damaged by ground subsidence due to the earthquake and estimated maximum MMI was 9. In the study area, around 4 kilometers of subsidence and road damage has occurred. According to geologic columnar section of this area (Consulting company of Utsuki Geo

Solution), ground contains organic soil, clay and silt with very small N values, and sand with N values of 10 or less are deposited to a depth of 12 to 20 meters. And also, the layer of peat or organic soil is deposited around 2 to 3 meters close to the surface. Reported subsidence location was consistent with the location of the Toho subway lines. It can be considered that subsidence and damage was concentrated on the subway line. The location map of study area with ground subsidence site are shown in Figure 5.

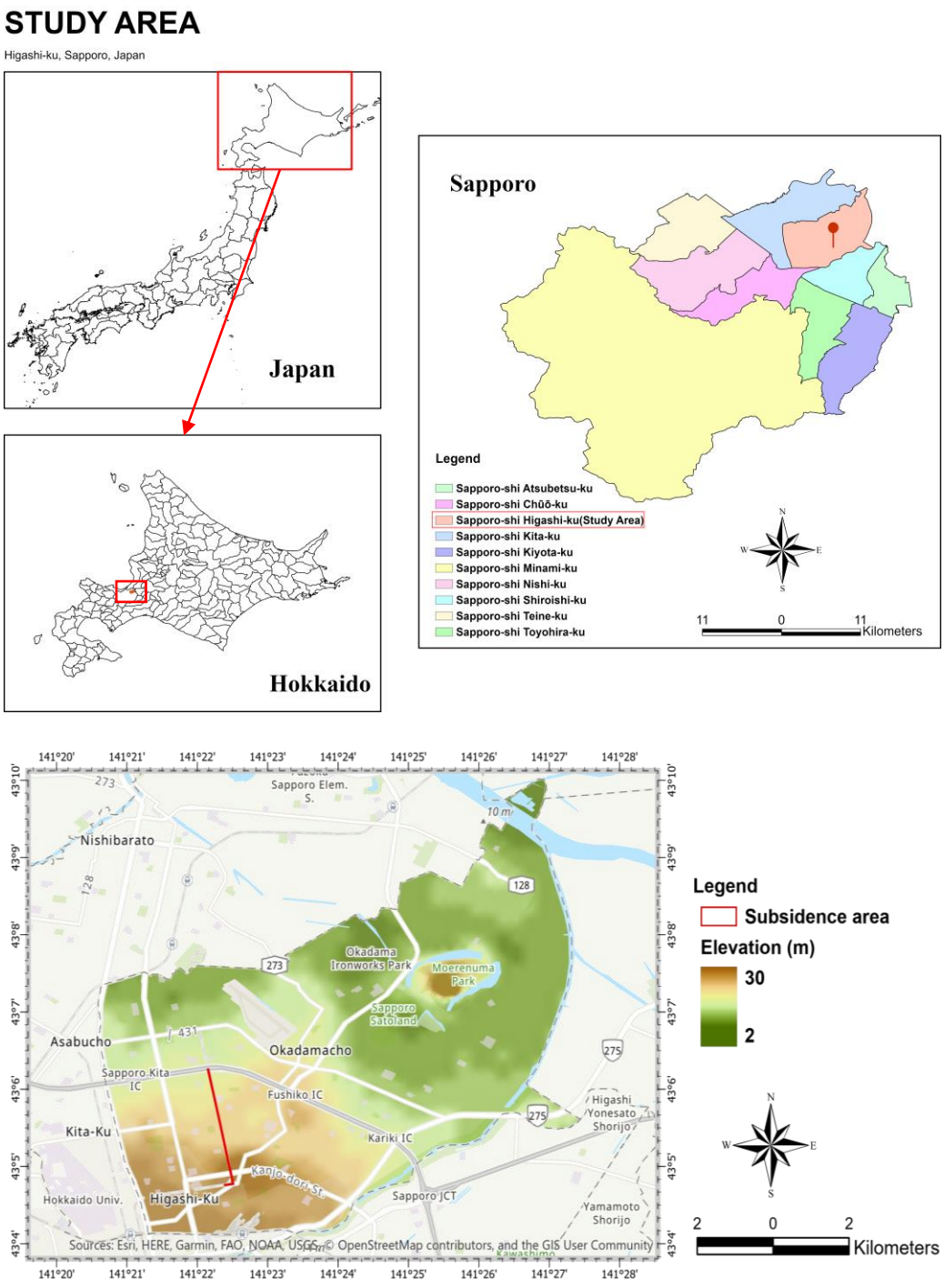

Figure 5. Higashi-Ward with ground subsidence location map.

3.1.2 Kiyota-Ward of Sapporo

Kiyota-Ward is located in the southeast part of Sapporo city in Hokkaido, Japan and total study area is 59.87 km2. Study area lies between 42°56'2"N - 43°0'25"N and 141°24'36"E - 141°26'2"E. Hokkaido is one of the most earthquake-prone areas and in the past 10 years (2010 ~ 2020) there were 56 earthquakes have occurred which are magnitude over 5 (Meteorological agency of Japan). Also, these frequent earthquake events have affected to the ground subsidence in Hokkaido, including study area. There was a major earthquake on September, 2018 which is called 2018 Hokkaido Eastern Iburi earthquake (M6.7) in around Iburi Subprefecture, southern Hokkaido. This earthquake caused serious damage of human lives and properties including infrastructures. Kiyota-Ward was also damaged by ground subsidence that influenced by the earthquake (Maximum MMI, 8). Reported locations of ground subsidence in the study area were distributed to over a wide area in residential area. Not as much as subsidence damage caused by 2018 Eastern Iburi earthquake, ground subsidence has occurred in the same area affected by another past earthquake (2003 Tokachi-oki earthquake). The thematic map of study area and investigated actual ground subsidence sites are presented in Figure 6. Residential area in Kiyota-Ward is composed with volcanic ash soil on the hilly area by using cut and fill method. The volcanic ash soil is already known as vulnerable to earthquake and ground subsidence. Thus, this indicates that housing complex in the study area is prone to liquefaction influenced by earthquake.

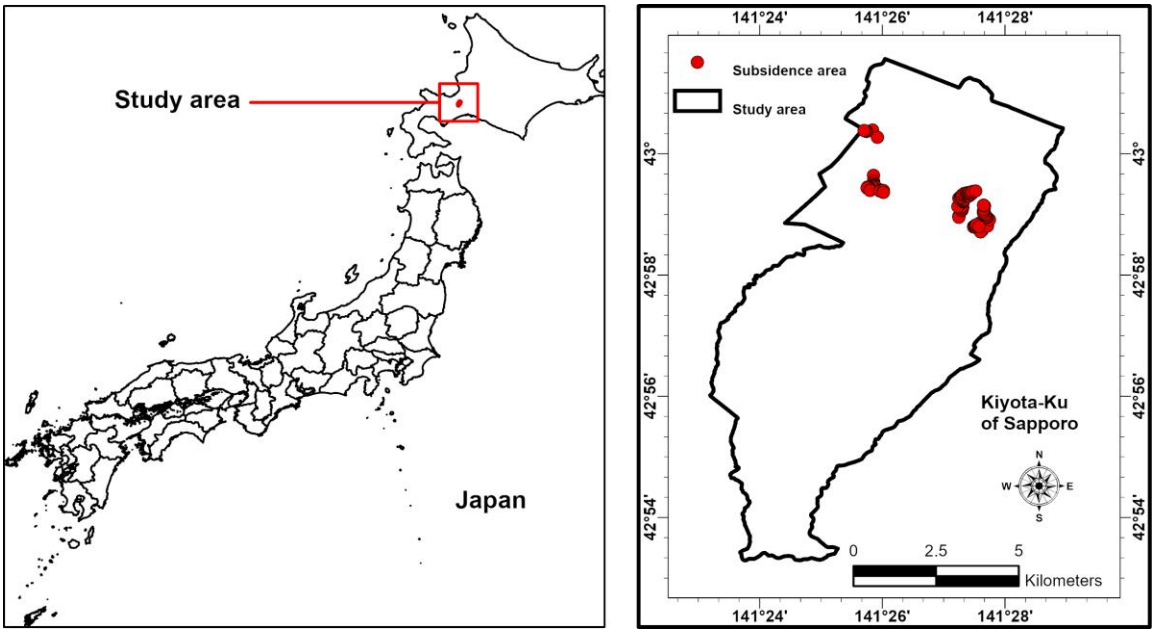

Figure 6. Kiyota-Ward and location of ground subsidence.

3.1.3 Sapporo

Sapporo is biggest and highly populated city in northern Japan and located in southwest of Hokkaido. Total area is 1,121.12 km2 and lies between 42°46'51"N (south) - 43°11'22"N (north) and 141°30'19"E (east) - 140°59'25"E (west). Sapporo has 10 administrative wards including: Atsubetsu, Chuo, Higashi, Kita, Kiyota, Minami, Nishi, Shiroishi, Teine and Toyohira (Figure 7). Population of study area has been growing annually and now is around 1.89 million as 5th highly populated city in Japan. Earthquake is a most common natural hazards in Japan and including around Hokkaido. Every year, lots of earthquake events occurring in various degree of magnitude and there were over 86 earthquake events had occurred which at least magnitude over 4 in around Hokkaido in the past ten years (Meteorological agency of Japan). On September in 2018, one of Japanese major earthquake has occurred in around Hokkaido. This earthquake was

named as “2018 Hokkaido Eastern Iburi earthquake” by meteorological agency of Japan. Due to the effects of this earthquake, land subsidence has occurred in Higashi and Kiyota ward of Sapporo. More specifically, subsidence sites in Higashi ward were occurred intensively on the road above the subway line. In Kiyota ward, subsidence has occurred in many places of building site (consist with residential area). Locations of ground subsidence in study area are given in Figure 7.

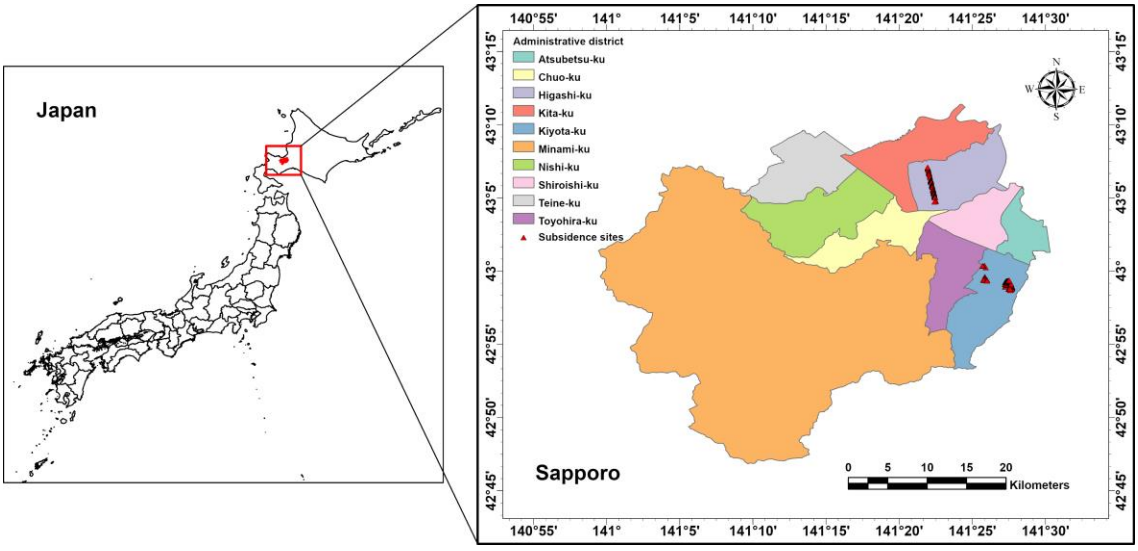

Figure 7. Administrative districts of Sapporo and ground subsidence sites.

3.2 Methodology

The flow of methodological approach in the current study has following five steps as presented in Figure 8.

(1) From investigated ground subsidence sites information produced by report of Japanese Geotechnical Society, ground subsidence location map was prepared as point data.

(2) Also, layers of all selected seven ground subsidence conditioning factors were constructed as polygon, line and point type data.

(3) Correlation between ground subsidence and related factors and weightage for all factors were identified using frequency ratio model.

(4) Overlay analysis was conducted and 3 thematic layers were constructed using 6 subsidence trigger factors. Then, earthquake-induced ground subsidence vulnerability map was constructed using GIS technique.

(5) Predicted susceptibility map was compared with prepared ground subsidence location map to evaluate the performance of this model using area under curve (AUC).

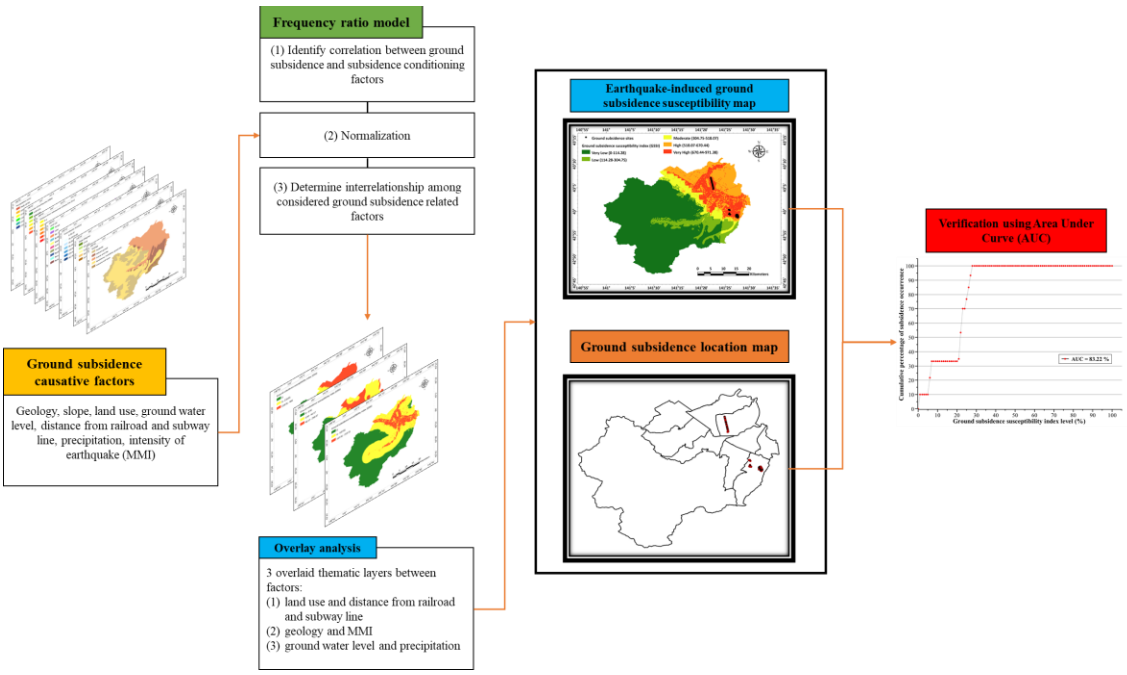

Figure 8. Flowchart of adopted methodology in current study.

3.3 Ground Subsidence Conditioning Factors

Many studies have identified major factors that causing ground subsidence in mine site or abandoned mines (Singh and Dhar, 1997; Waltham, 1989). However, important factors are not yet clearly defined regarding ground subsidence in urban areas. In this study, to identify major factors that contribute to ground subsidence and to evaluate ground subsidence susceptibility in the study area, seven conditioning factors were selected. Considered seven factors are including geology (lithology), slope, land use, ground water level, distance from railroad, precipitation and intensity of earthquake (MMI). Geology, slope, land use, railroad and precipitation databases were collected from geological map, topographic map, land use map, railroad map and climate data provided by National Land Information Division (MLIT of Japan). Factor of land use was divided into 8 subclasses as shown in Figure 9-11. MMI data was collected as point data of 20 nearest regions from study area based on the earthquake information provided by meteorological agency of Japan and constructed as a layer using inverse distance weighting (IDW) interpolation method. Ground subsidence area where occurred by Eastern Iburi earthquake was collected using Google Earth Pro with data of location information from final report of ground subsidence disaster investigation team (Japanese Geotechnical Society). Then, this file was converted to GIS database format (polygon and point) using ArcGIS Pro software. Constructed ground subsidence area data was used for EGSSM mapping and verification of prediction accuracy. Constructed layers of each factor are listed in Table 3 and presented in Figure 9-11.

Table 3. Considered seven conditioning factors and location of ground subsidence.

Factors	Data type	Data source
Ground subsidence area	Polygon and Point	Japanese Geotechnical Society
Geology, Lithology	Polygon	National Land Information Division (MLIT of Japan)
Slope	Polygon	
Land use	Polygon	
Ground water level	Point	Borehole database (Utsuki Geo Solution)
Distance from railroad	Line	National Land Information Division (MLIT of Japan)
Precipitation	Polygon	
MMI	Point	Meteorological agency of Japan

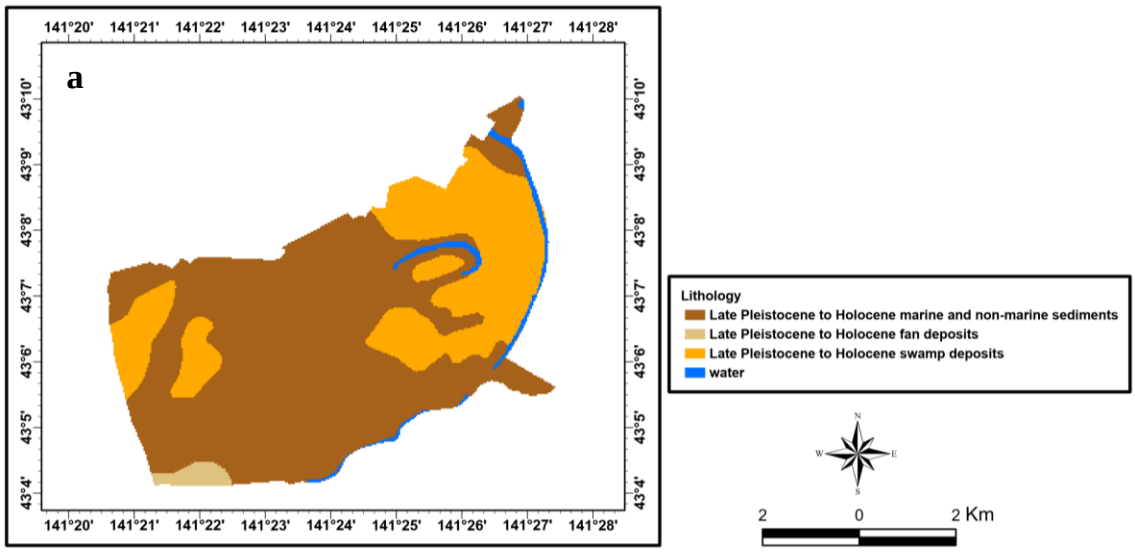

Figure 9. Constructed data of each factor for Higashi-Ward. **a** lithology, **b** slope, **c** land use, **d** ground water level, **e** distance from railroad and subway line, **f** precipitation **g** MMI.

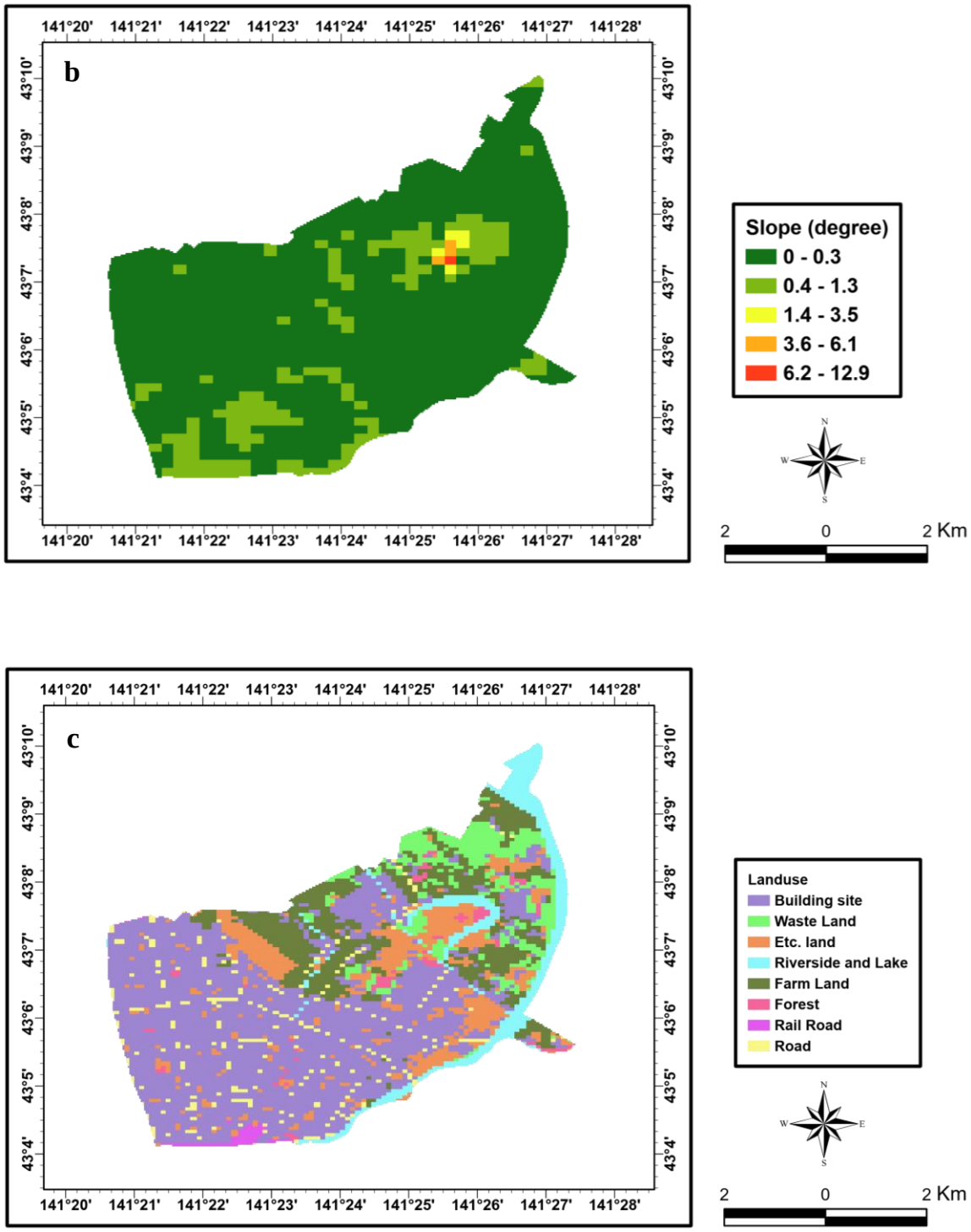

Figure 9. (continued)

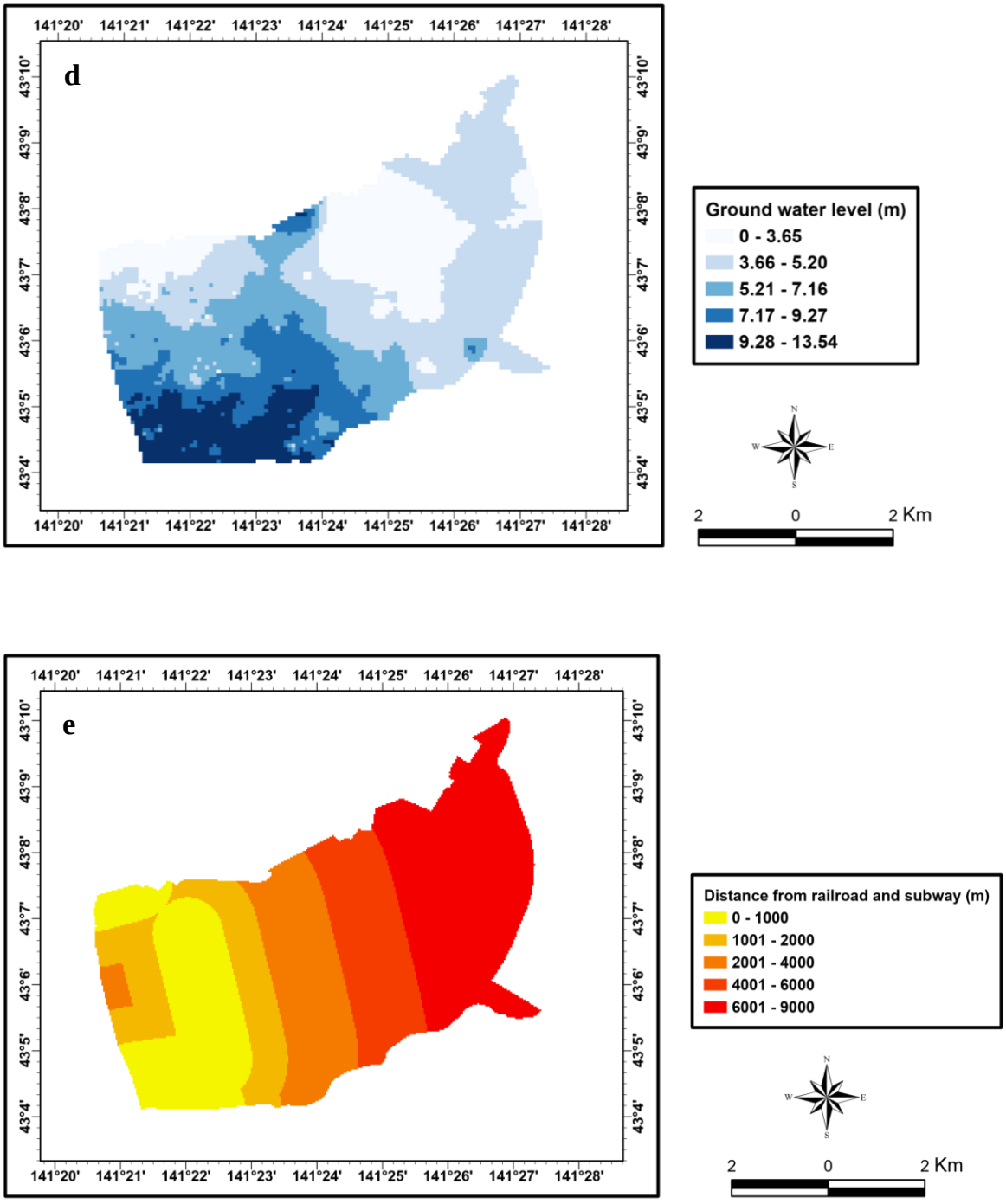

Figure 9. (continued)

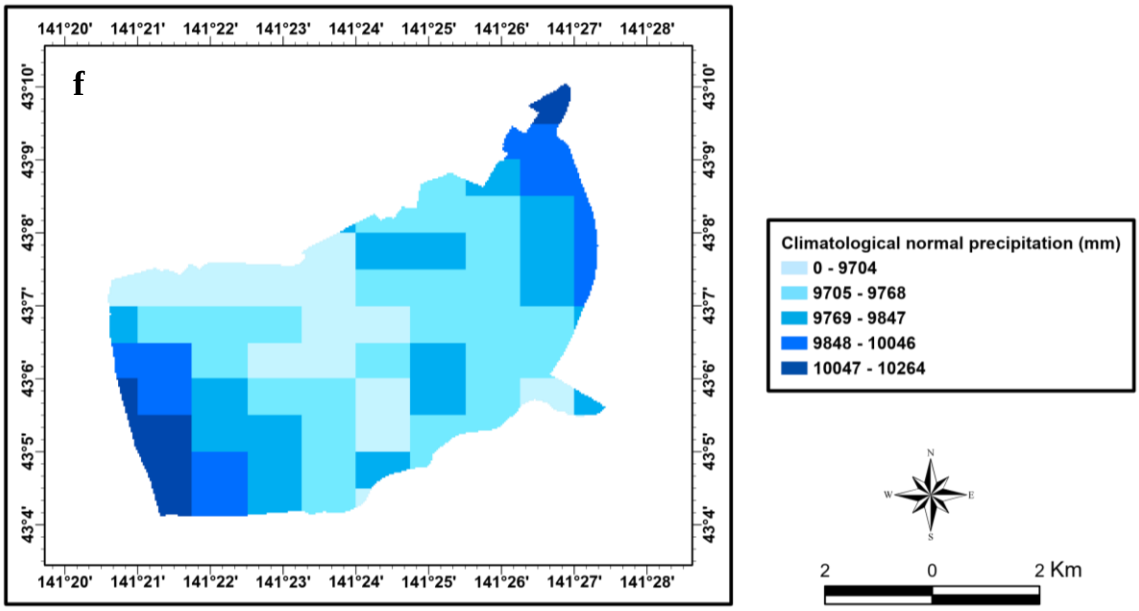

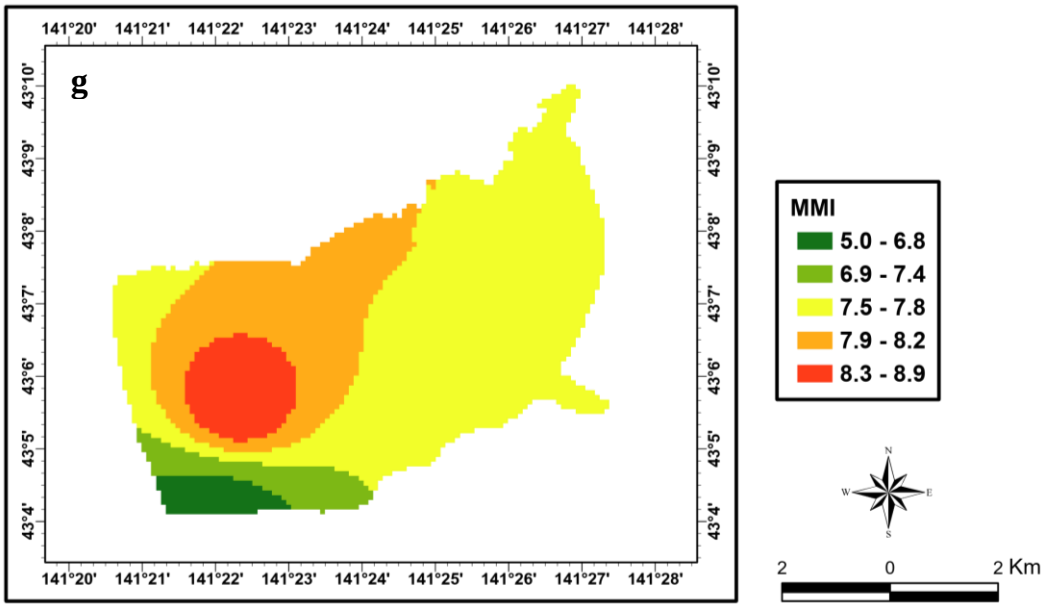

Figure 9. (continued)

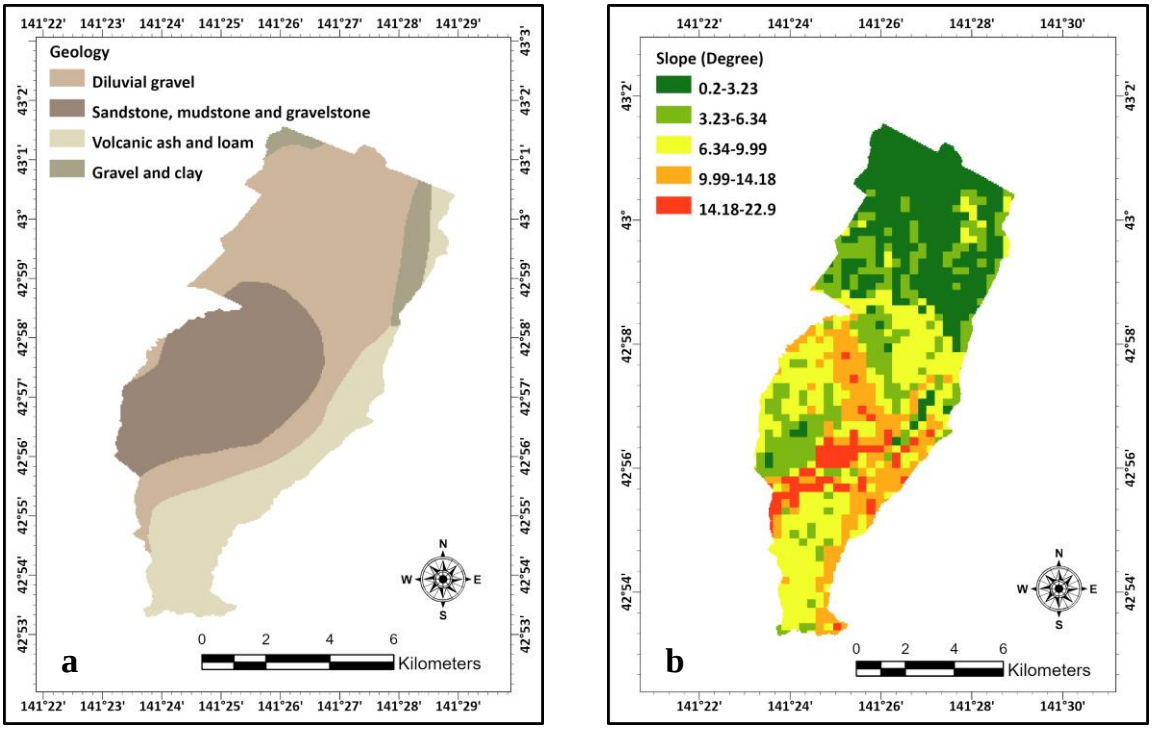

Figure 10. Thematic layers of ground subsidence trigger factors for Kiyota-Ward. **a** geology, **b** slope, **c** land use, **d** ground water level **e** distance from railroad, **f** precipitation, **g** MMI.

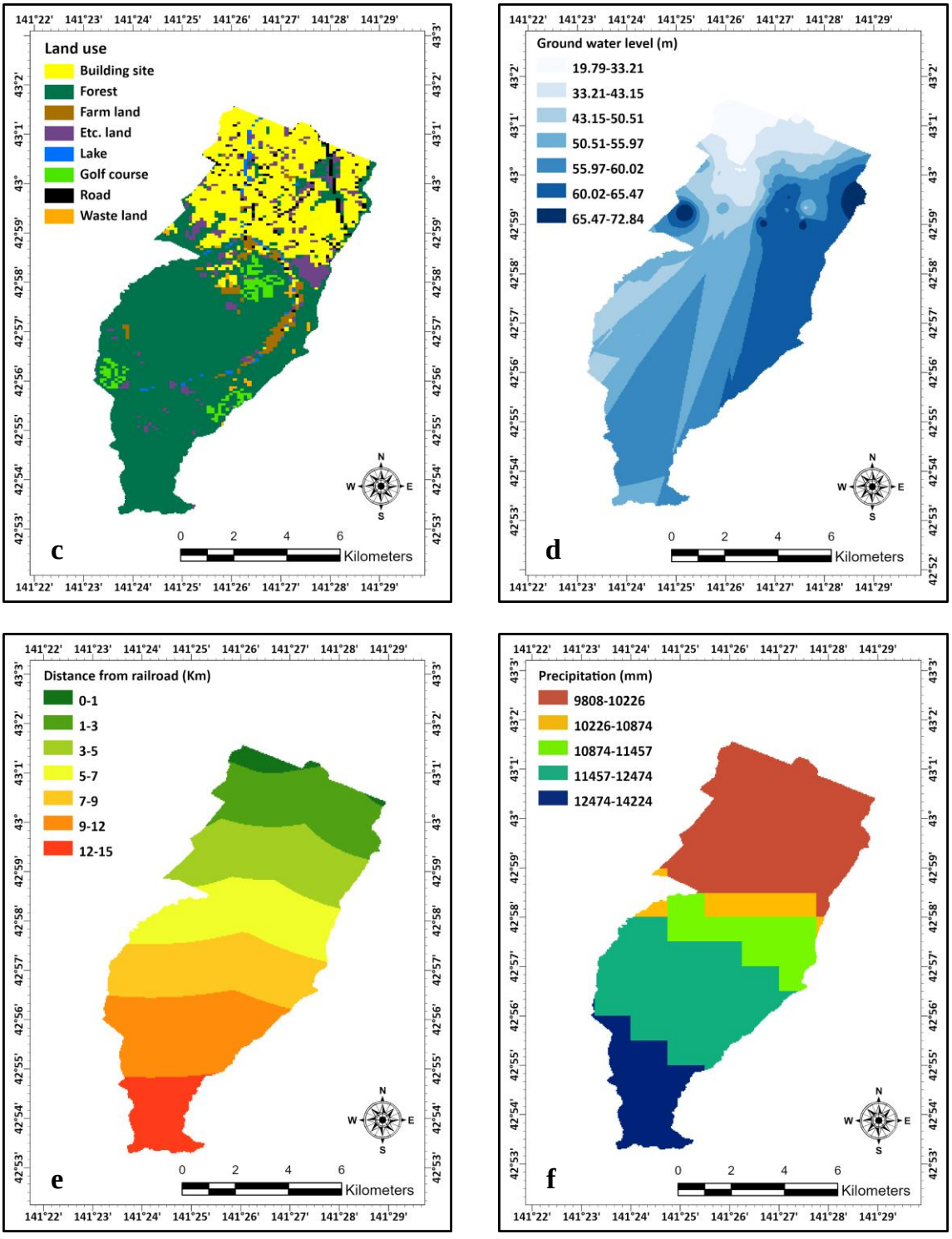

Figure 10. (continued)

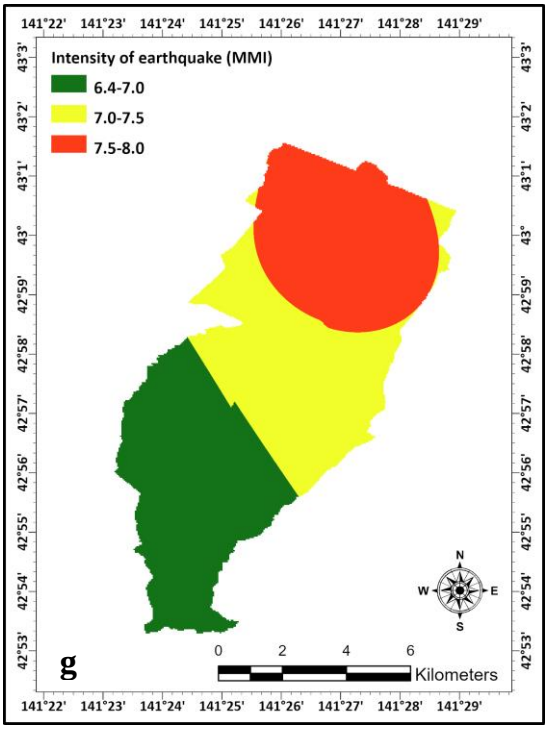

Figure 10. (continued)

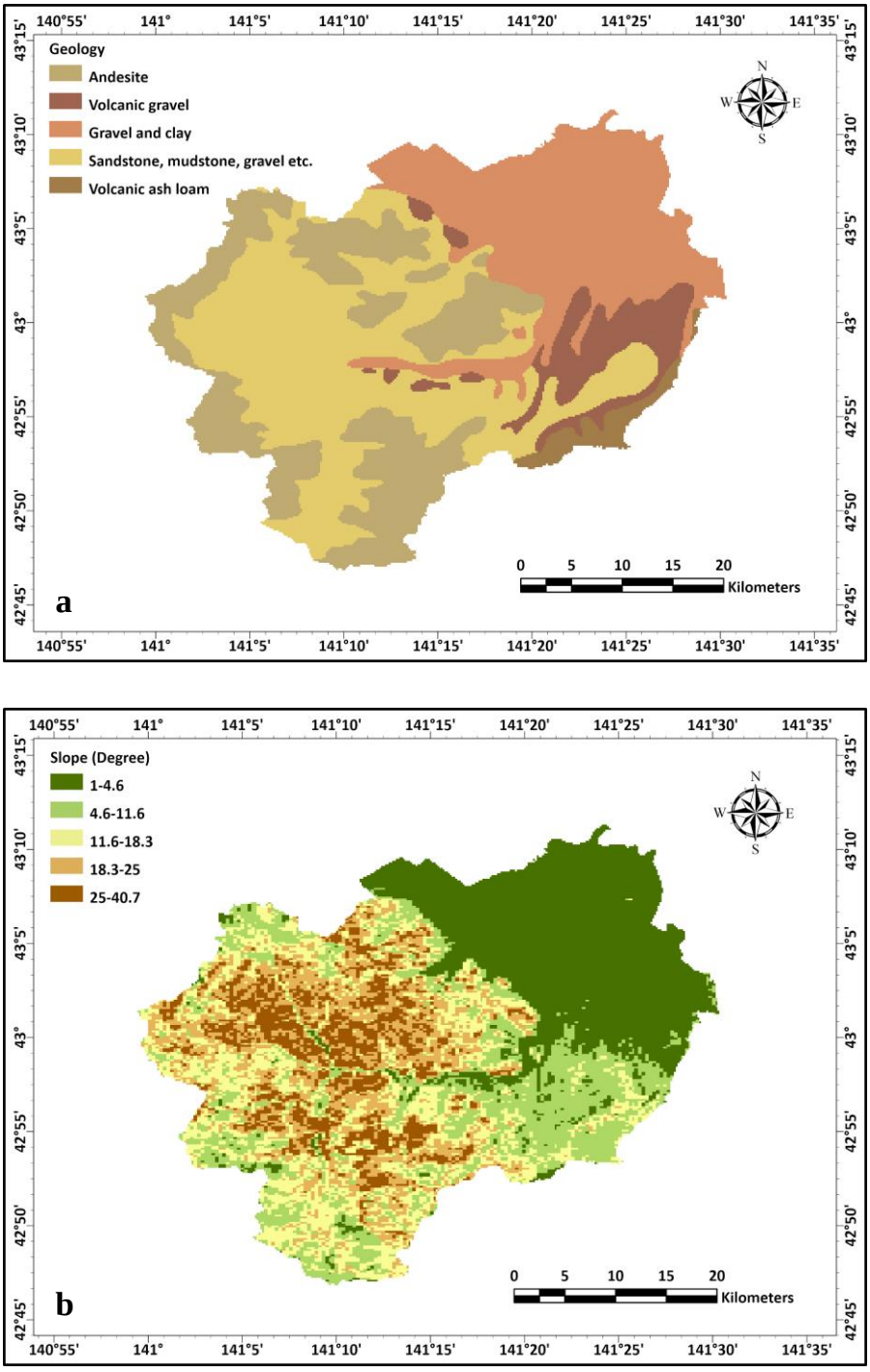

Figure 11. Thematic layers of ground subsidence trigger factors for Sapporo. **a** geology, **b** slope, **c** land use, **d** ground water level **e** distance from railroad, **f** precipitation, **g** MMI.

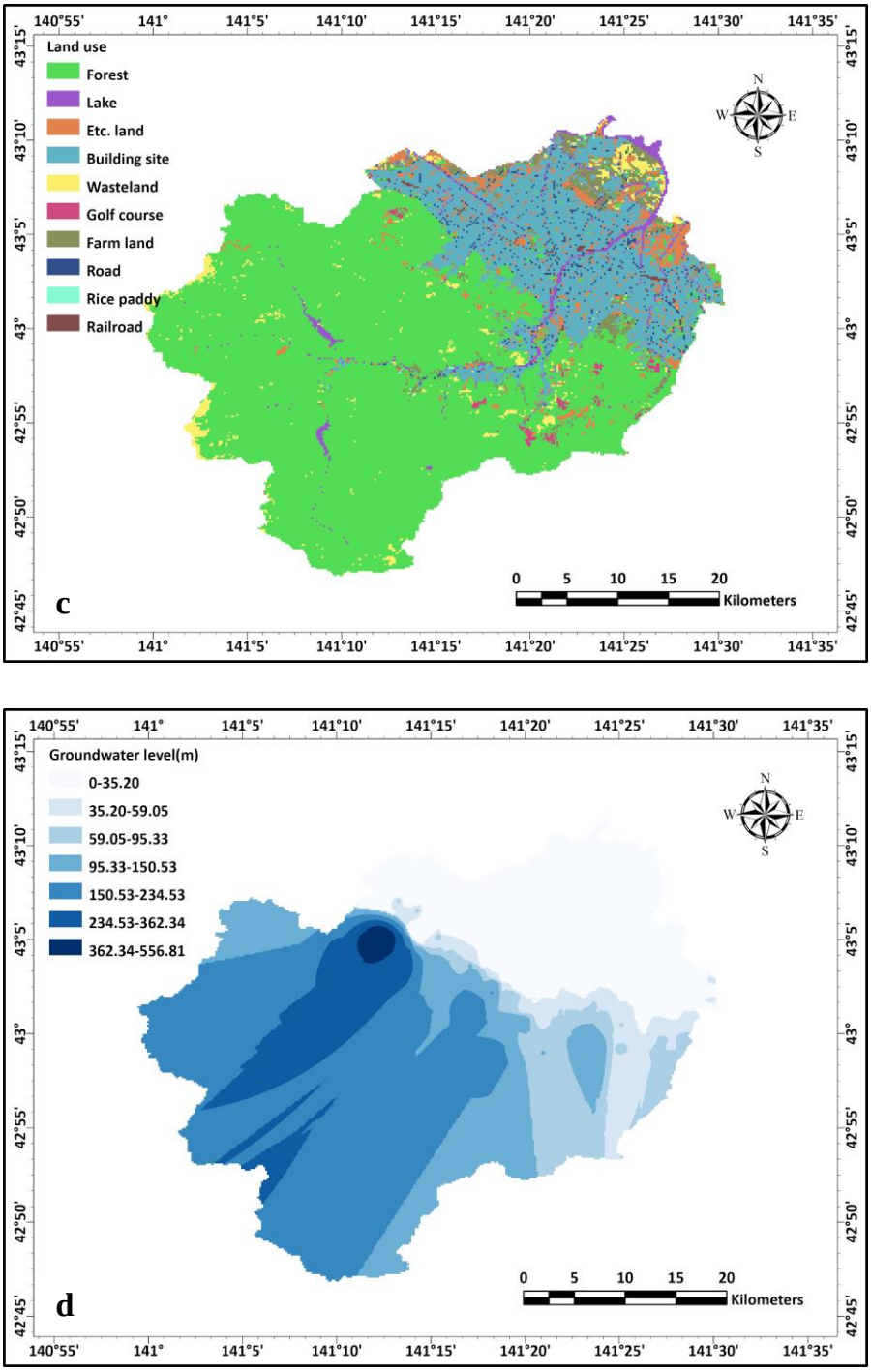

Figure 11. (continued)

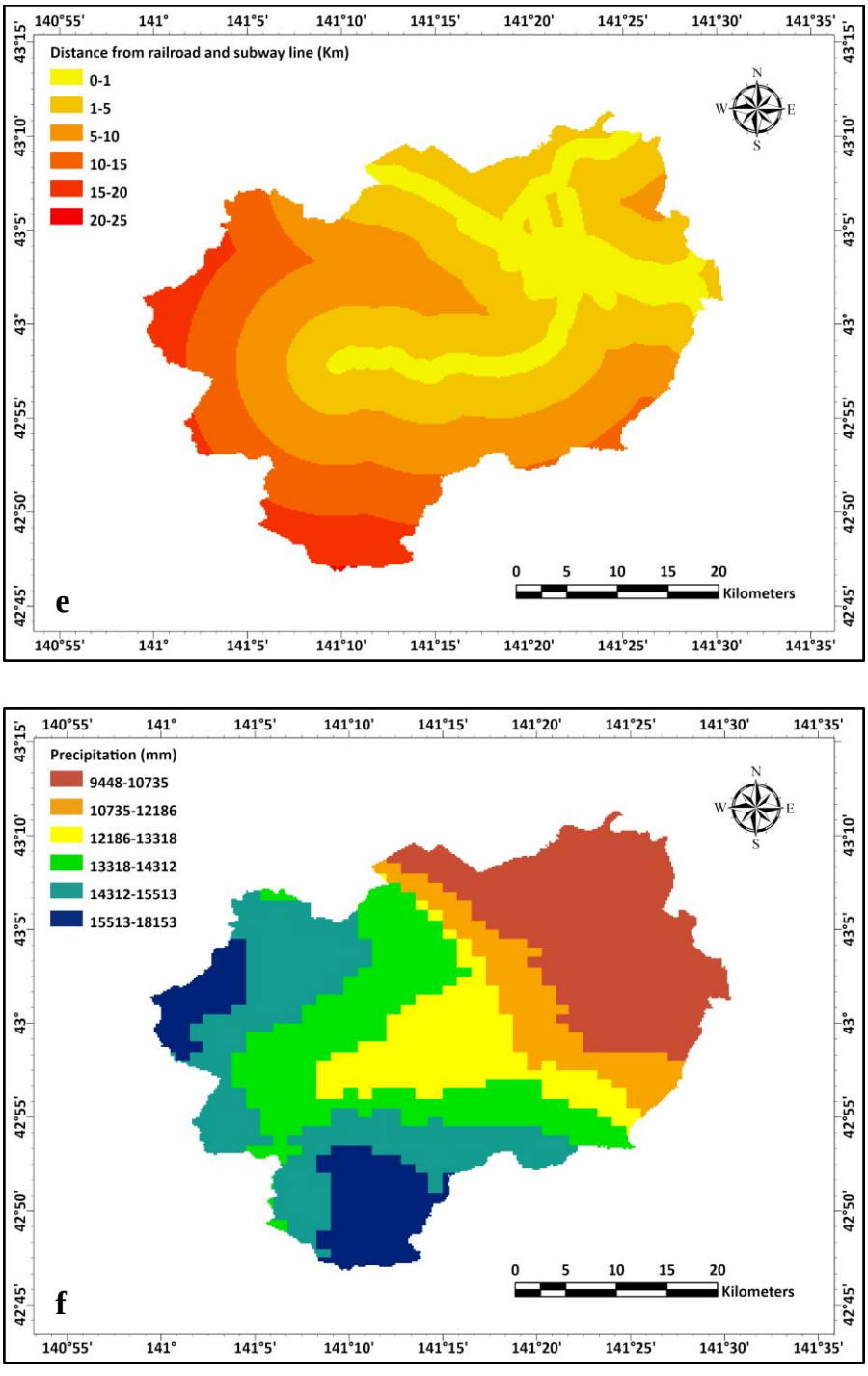

Figure 11. (continued)

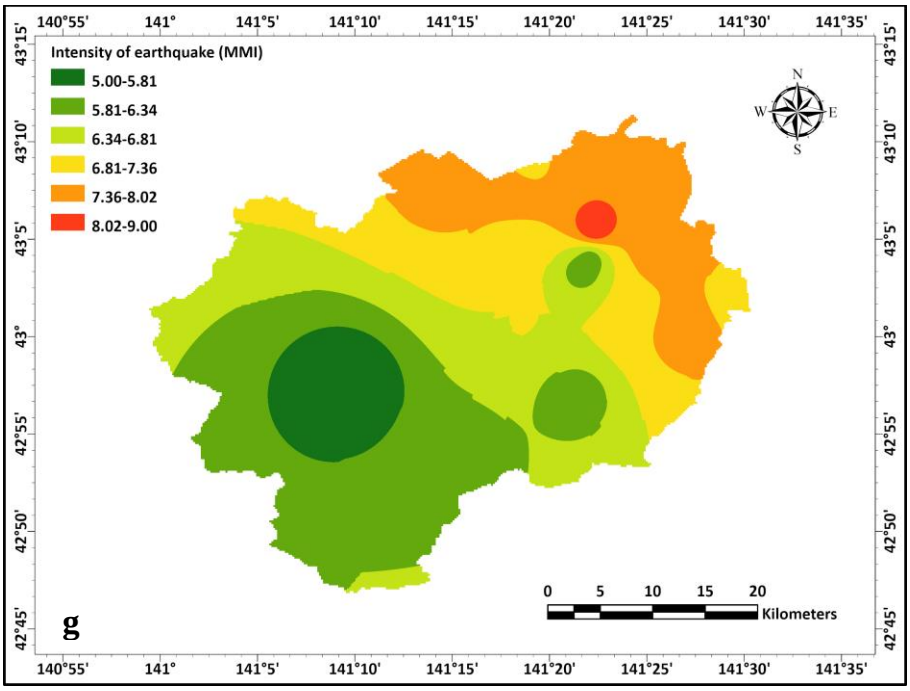

Figure 11. (continued)

3.4 Borehole Database

Information from the borehole is essential to identify and evaluate the earthquake-induced soil liquefaction (Lu et al. 2017 and Lai et al. 2020). The damage risk from earthquake-induced ground subsidence is critical to big cities more than rural areas. Thus, it is very important to secure and utilize abundant borehole data for assessment of ground subsidence susceptibility in urban areas.

In this study, borehole databases of Sapporo produced by Consulting company of Utsuki Geo Solution were used for preparing data of ground water level. Also, these data were used for understanding geological deposition close to the surface for study area.

Normally, it is hard to get borehole databases for urban areas. However, for the purpose of risk reduction and management in urban areas, researchers can get the borehole data from reliable agencies or companies. Moreover, by gathering borehole databases for other main cities not only Sapporo and systemizing it by sum of all the data, it can be applied approach of this study for real situation, more properly. Figure 12 shows flow of ground water level data extraction from raw databases (borehole data) and Figure 13 shows the location of boreholes. For the first step, only ground water level data was extracted from 3D type of borehole data and arranged as a table with information of longitude, latitude and ground water level (m) for Sapporo using Excel software. Extracted total number of data were 4,814 for entire area of Sapporo city. Then, inverse distance weighting (IDW) interpolation method was used with 4,814 ground water level data using ArcGIS software. From the results of IDW method, data was re-extracted for constructing GIS database of target areas using clip tool in ArcGIS Pro. Finally, layer of ground water level for study area was constructed with 605 borehole databases for Higashi-Ward, 134 borehole databases for Kiyota-Ward and 4,814 borehole databases for entire area of Sapporo city.

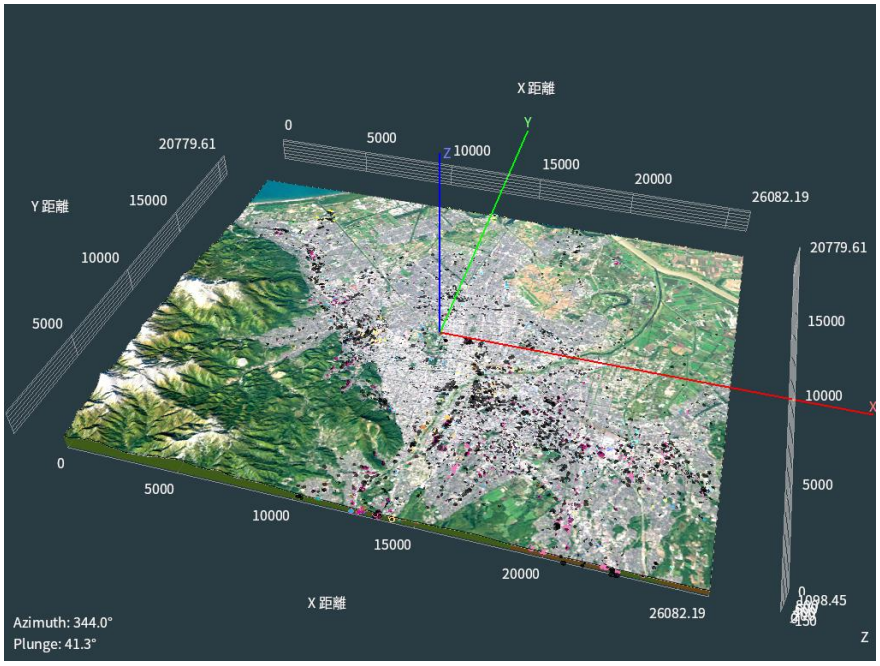

(a) Raw data (borehole data)

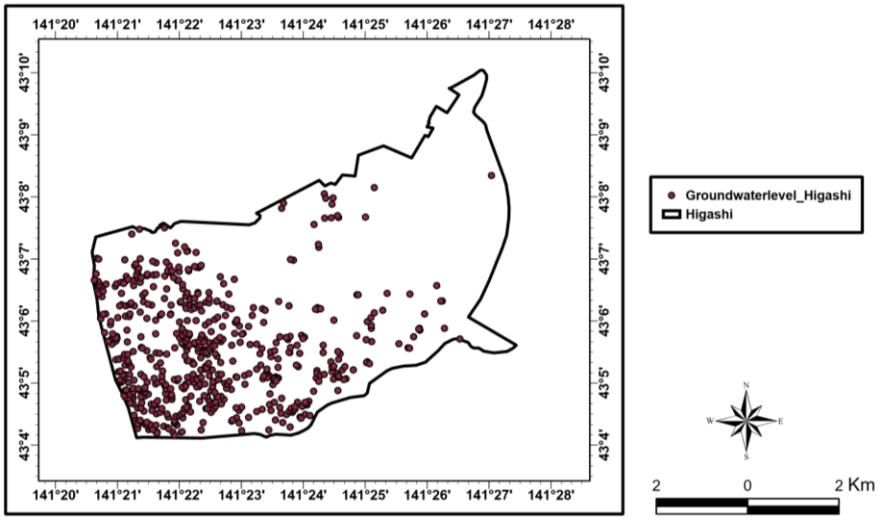

(b) Extracted data of target area

Figure 12. Flow of construction for GIS databases from raw data.

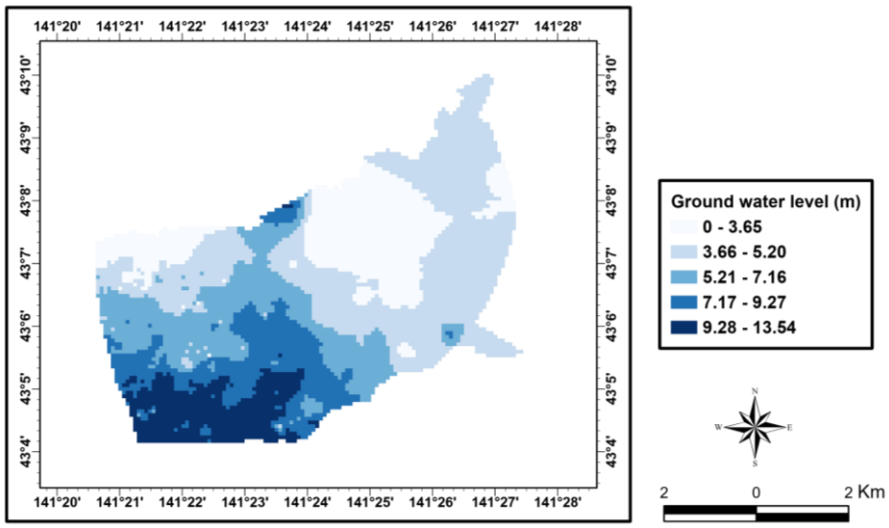

(c) Constructed GIS database

Figure 12. (continued)

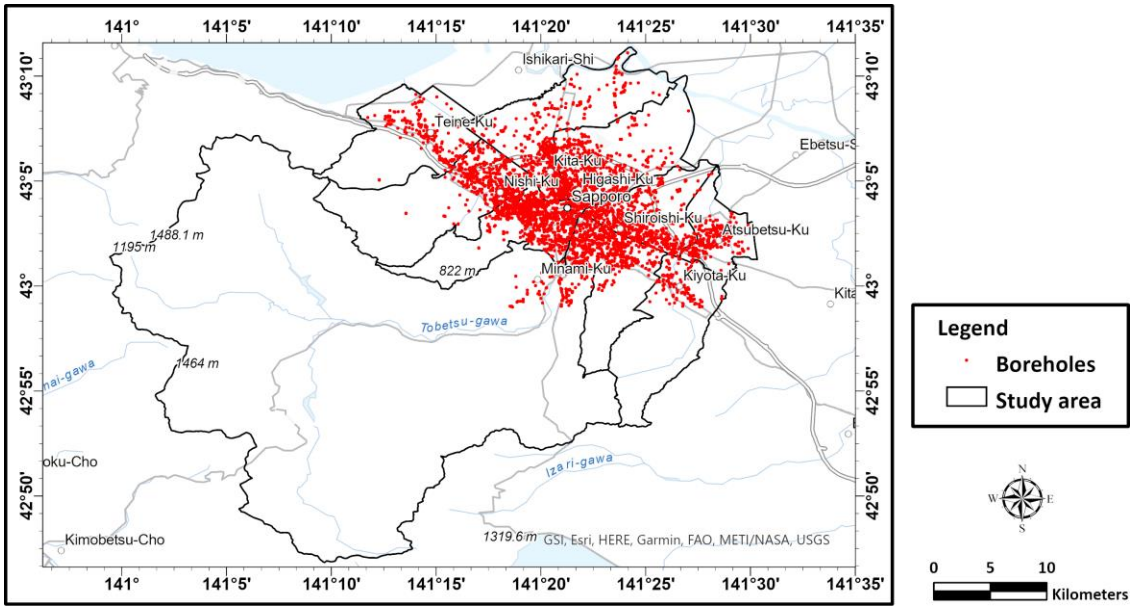

Figure 13. The location map of original borehole databases.

3.5 Analysis Methods

3.5.1 Frequency Ratio Model

Frequency ratio model is a quantitative and probability analysis method which is frequently and widely used with reliable results to assess and predict the susceptibility of disasters (Ding et al. 2017; Yalcin et al. 2011; Cao et al. 2016; Lee and Park. 2013; Arabameri et al. 2021). The strength of FR model is, it could be applicated easily with simple calculation to the assessment of vulnerability index of hazard risks. In addition, this method has great interconvertible with GIS technique which is now widely used around the world (Intarawichian and Dasananda, 2011; Oh and Lee, 2011).

Relationship between conditioning parameters and ground subsidence area is important for the evaluation of ground subsidence susceptibility. And this relationship could be considered from relationship between conditioning parameters and the areas where ground subsidence has not occurred (Rasyid et al. 2016). To analysis this co-relationship, frequency ratio approach was applicated in this study.

FR values of each factor were calculated by using Eq 1.

$$FR = \frac{P(sf) \,/\, \sum SP}{P(cf) \,/\, \sum CP} \tag{1}$$

where, *P(sf)* number of pixels of ground subsidence within class c of factor f, $\sum SP$ total pixels of ground subsidence area, *P(cf)* number of pixels in class c of factor f, and $\sum CP$ total pixels of the area.

Calculated FR values are normalized from 0 to 1 by dividing FR of classes within a factor by total FR of the factor. This normalized ratio value is the relative frequency (RF) and RF has defection that consider all conditioning factors as equal weight. To solve this problem and also consider mutual interrelationship among selected factors (weights of individual factors related with ground subsidence), prediction rate (PR) was calculated (Acharya and Lee, 2019; Ullah and Zhang, 2020).

$$PR = \frac{(Max\ RF - Min\ RF)}{(Max\ RF - Min\ RF)Min\ RF} \quad (2)$$

Using PR values, ground subsidence susceptibility index (GSSI) was calculated by combining PR values of each factor and RF values of each class as below:

$$GSSI = \sum INT(RF_c) * PR_f \quad (3)$$

where, RF_c RF values of each class within factor, PR_f PR values of each factor.

FR indicates subsidence occurred areas to the total areas of the study. FR value of 1 means the average and higher FR value than 1 indicates that the conditioning factor has a higher influence on ground subsidence. Lower FR value than 1 means the parameter has lower influence on ground subsidence (Akgun et al. 2008; Khan et al. 2019). And calculated GSSI was utilized for the construction of EGSSM.

3.6 Validation Method

3.6.1 Area Under Curve (AUC)

The predicted result on potential risk of earthquake-induced ground subsidence in study area was verified using area under curve (AUC) method which is widely used to assess the performance of prediction models. (Bradley, 1997). Accuracy of prediction result was evaluated by comparing constructed ground subsidence vulnerability map with investigated past ground subsidence areas. For this, subsidence susceptibility indices were used to draw the rate curve. All grid indices in the study area were reclassified in descending order to generate this rate curve. In the next step, as cumulative 1 percent intervals, the reclassified grid values were divided into 100 classes. Generated rate curve indicates how well the considered trigger factors and applicated model predict the potential ground subsidence. As a consequence, the area under the curve approach can be used to evaluate the prediction accuracy, qualitatively. (Lee and Dan, 2005; Lee et al. 2012). Then, area under curve was calculated to compare the results.

Chapter IV

Results and Discussion

4.1 Analysis results of ground subsidence susceptibility in Higashi-Ward

4.1.1 Probability of ground subsidence

FR values of all seven factors were calculated by using frequency ratio model as shown in Table 4. Considered seven factors in this study are lithology, slope, land use, ground water level, distance from railroad and subway line, precipitation (Rainfall) and intensity of earthquake (MMI). Also, to analysis weightage for seven factors and construct ground subsidence susceptibility map PR values were calculated from RF.

In the case of lithology, only class of Late Pleistocene to Holocene marine and non-marine sediments had FR over 1 (1.07) and this result indicates having high ground subsidence probability. Also, FR of Late Pleistocene to Holocene swamp deposits class had FR value of 0.96 and it indicates less probability to ground subsidence than FR value greater than 1. Rest classes had FR value of 0.24 and 0, respectively which means low probability or no likelihood of ground subsidence.

For degree of slope, higher FR values were shown as gradient increased up to 1.3 and peak FR value was 1.98 at degree of 0.4 to 1.3. Results of gradient from 1.4 to 12.9 were indicated very low probability of ground subsidence in the study area.

Land use is an important factor regarding ground subsidence hazard in the urban area, because of the risk of damage of properties and human lives is high. Land use factor was divided into subclasses as building site, waste land, etc. land, riverside and lake, farm

land, forest, railroad and road. Among the classes, railroad and road classes were denoted very high subsidence probability had FR of 15.78 and 7.69, respectively. Also, the FR values were greater than 1 in the class of building sites, farm land and forest. This result indicates, at railroad and road are more prone to ground subsidence than other land use sites in this study area.

Subsidence probability for ground water level, had high FR values at 5.21-7.16 and 7.17-9.27 m with ratio of 2.38 and 2.21, respectively and this denotes that high probability of ground subsidence at this range of ground water level.

For distance from railroad and subway line, only had highest FR value of 2.77 from 0 to 1,000 m and denoted very low probability over 1,000 m. This result indicates susceptibility of ground subsidence is higher as closer to railroad or subway line. Also, this result shows agreement with reported actual ground subsidence area information.

In the case of precipitation, data of three-decade averages of climatological variables were used. FR values were higher as precipitation increase within range 0 to 9,847 mm. And indicated highest probability of subsidence at the range of 9,769 to 9,847 mm which had FR value of 2.42.

For MMI, as intensity of earthquake increase, the FR values denoted higher from range of 7.5 to 8.9 in the area. Highest FR value of 12.47 were for class of 8.3 to 8.9 and this result indicates very high ground subsidence probability.

Table 4. FR values for all classes of each factor for Higashi Ward.

Factor	Classes	Class pixels (%)	Subsidence Pixels (%)	FR
Lithology	Late Pleistocene to Holocene marine and non-marine sediments	66.50	71.45	1.07
	Late Pleistocene to Holocene fan deposits	2.52	0.60	0.24
	Late Pleistocene to Holocene swamp deposits	29.07	27.95	0.96
	water	1.91	0.00	0.00
Slope (Degree)	0-0.3	87.74	80.48	0.92
	0.4-1.3	9.85	19.52	1.98
	1.4-3.5	1.55	0.00	0.00
	3.6-6.1	0.59	0.00	0.00
	6.2-12.9	0.27	0.00	0.00
Land use	Building site	46.90	52.67	1.12
	Waste land	10.45	3.62	0.35
	Etc. land	13.22	4.55	0.34
	Riverside and lake	23.89	4.50	0.19
	Farm land	1.81	1.88	1.04
	Forest	1.41	3.97	2.82
	Railroad	1.35	21.33	15.78
	Road	0.97	7.47	7.69

Table 4. (continued)

Factor	Classes	Class pixels (%)	Subsidence Pixels (%)	FR
Ground water level (m)	0-3.65	7.70	0.00	0.00
	3.66-5.20	53.02	15.22	0.29
	5.21-7.16	23.19	55.21	2.38
	7.17-9.27	13.39	29.57	2.21
	9.28-13.54	2.70	0.00	0.00
Distance from railroad and subway line (m)	0-1,000	36.05	100.00	2.77
	1,001-2,000	25.76	0.00	0.00
	2,001-4,000	7.76	0.00	0.00
	4,001-6,000	15.98	0.00	0.00
	6,001-9,000	14.44	0.00	0.00
Precipitation (mm)	0-9,704	36.12	17.24	0.48
	9,705-9,768	46.34	62.51	1.35
	9,769-9,847	8.35	20.25	2.42
	9,848-10,046	8.18	0.00	0.00
	10,047-10,264	1.01	0.00	0.00
MMI	5.0-6.8	2.42	0.00	0.00
	6.9-7.4	3.93	0.00	0.00
	7.5-7.8	60.29	16.34	0.27
	7.9-8.2	27.83	14.68	0.53
	8.3-8.9	5.53	68.98	12.47

4.1.2 Interrelationship between factors and ground subsidence

After preparation of all factor layers related with ground subsidence, to construct final ground subsidence susceptibility map of study area, PR value (weight) of each factor were calculated from prepared RF values using frequency ratio model. Table 5 shows calculated weight of each factor and weight rank. Highest rank of factor was Railroad and subway line and this means the factor has high influence to ground subsidence. MMI has second highest PR value after rank 1 factor. Slope and Precipitation have some influence to predict ground subsidence occurrence. Lithology, Land use and Ground water level have low contribution to subsidence than other 4 factors in this study.

Table 5. Weight of each factor and rank for Higashi Ward.

Factor	Rank	PR (Weight)	Factor	Rank	PR (Weight)
Lithology	7	1.00	Railroad and subway line	1	2.12
Slope	3	1.45			
Land use	5	1.13	Precipitation	4	1.21
Ground water level	6	1.03	MMI	2	1.99

4.1.3 Overlay analysis between conditioning factors

From these results, three thematic maps were constructed to analysis how the factors will be affected to prediction of final ground subsidence susceptibility as shown in Figures 14 to 16. This analysis was performed except for lowest weight data of lithology. Figure 14 shows GSSI of overlaid layers of land use and ground water level. Calculated GSSI values were from 0 to 109.33. In this map, GSSI values were high (values from

72.89 to 109.33) along the roads. Also, index from 36.44 to 72.89 was showed in the building sites with high ground water level. This result indicates that roads and building sites where located on the areas with high ground water level are more vulnerable to ground subsidence. And this information was reflected in the final EGSSM.

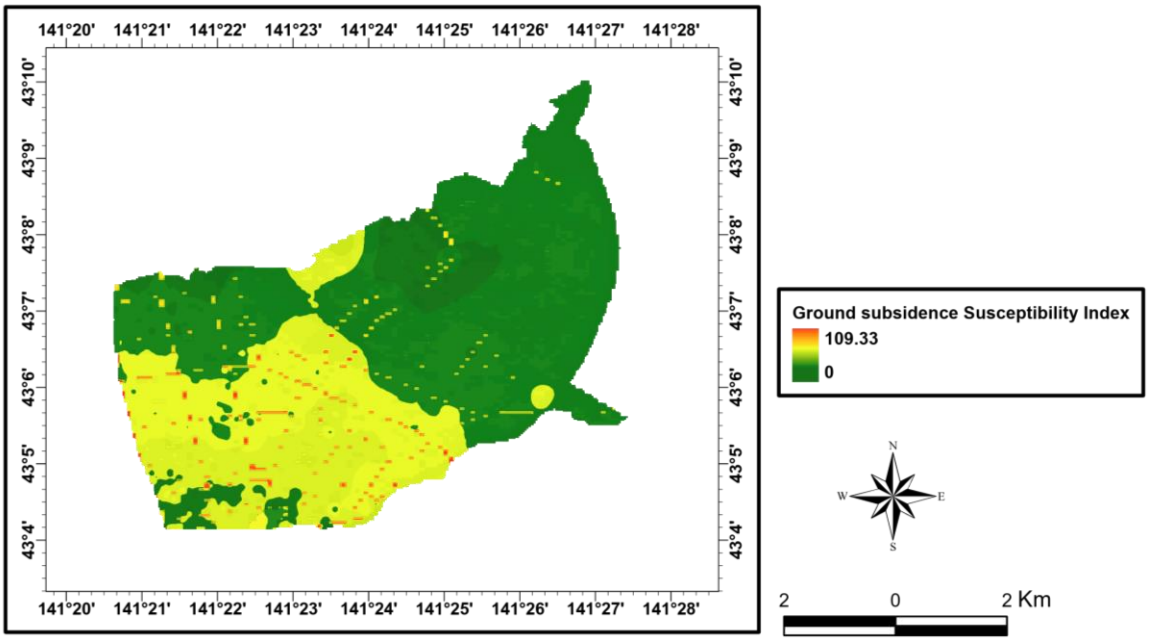

Figure 14. Result of overlay analysis between factor land use and ground water level.

Overlaid layers of slope and precipitation had GSSI values from 0 to 167.57 as shown in Figure 15. High GSSI values (111.71 – 167.57) were showed at very low degree of slope and areas with moderate amount of rainfall. But the entire of study area is a flat area with almost no slope and also there is not much precipitation, annually. For this reason, slope and precipitation had little effect on ground subsidence occurrence in this study.

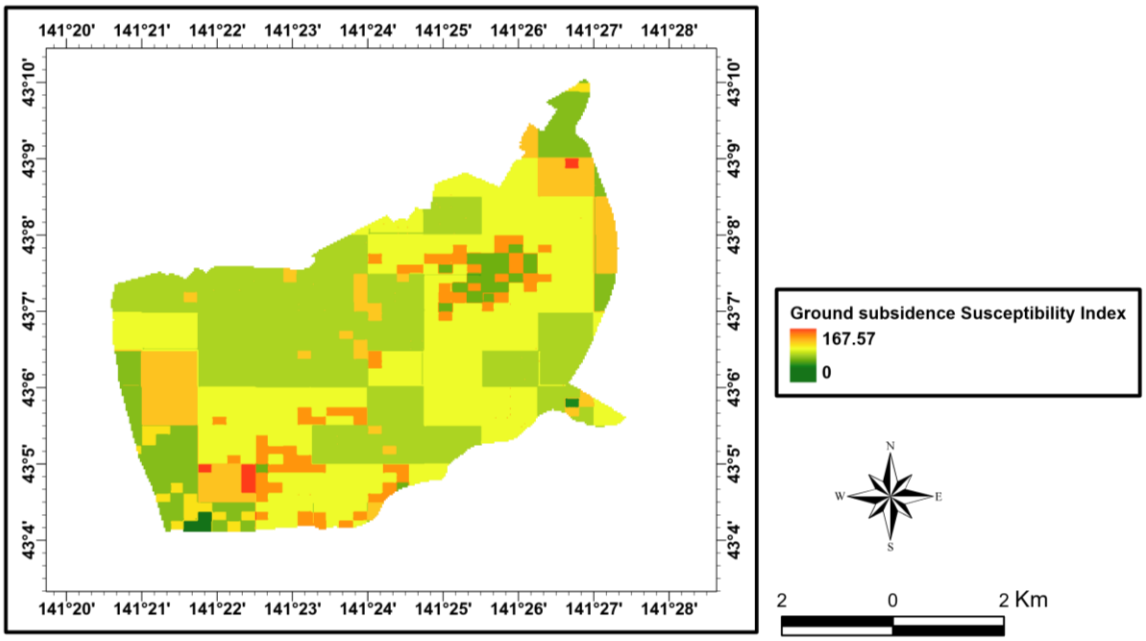

Figure 15. Result of overlay analysis between factor slope and precipitation.

Figure 16 shows overlaid factor layers of railroad and subway line and MMI. These two factors had highest weights among the seven factors and ground subsidence susceptibility index was from 0 to 397.07. This result showed the areas closer to railroad and subway line and had high intensity of earthquake are more prone to occur ground subsidence than other areas. Thus, it also showed that areas where farther from railroad and subway line and has low MMI are relatively has lower susceptibility index. Accordingly, this result had most influence to the construction of final ground subsidence susceptibility map.

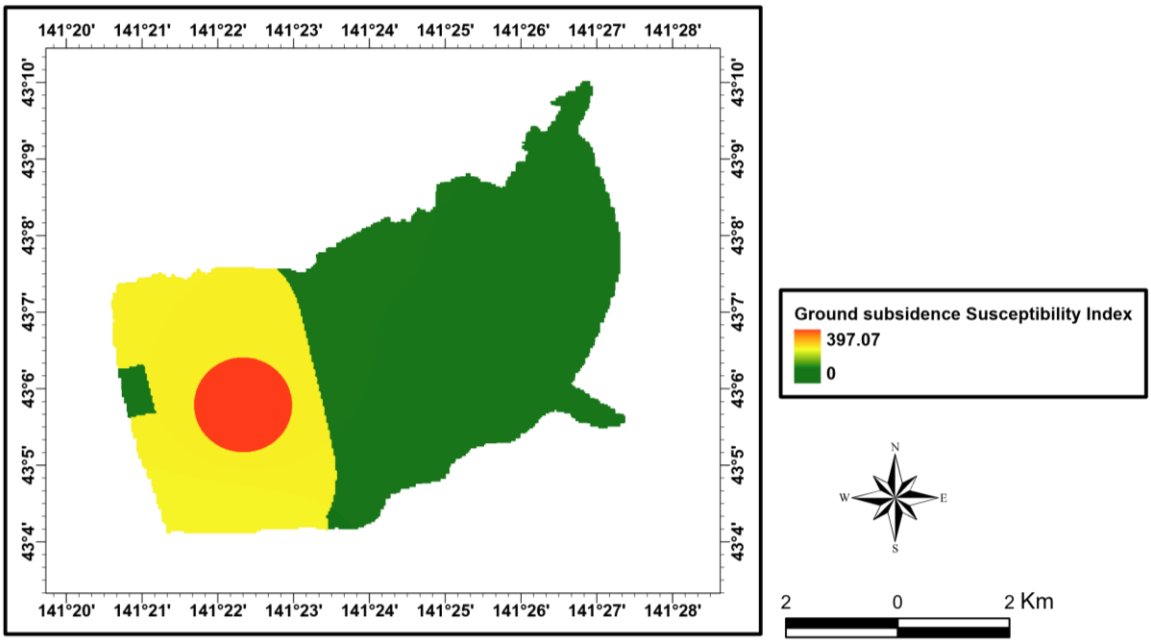

Figure 16. Result of overlay analysis between factor railroad and subway line and MMI.

4.1.4 Susceptibility map and validation

Using PR weight of each factor, GSSI was calculated by Eq. 3 and finally, ground subsidence susceptibility map was constructed as shown in Figure 17 using ArcGIS Pro 2.4.3 software. Range of ground subsidence susceptibility index was from 29. 38 to 635.33 in this study. Also, ground subsidence susceptibility index was divided in 5 classes as follow: Very low (29.38 - 149.77), Low (149.77 - 271.16), Moderate (271.16 - 392.55), High (392.55 - 513.94) and Very high (513.94 - 635.33). Results of verification are shown in Figure 18. This result indicates that, 49 % of all ground subsidence has occurred in 10 % of study area where having high ground subsidence susceptibility index rank. Also, in 25 % of study area, occurred 85.17 % of all ground subsidence and all of

ground subsidence has occurred in 40 % of study area. Calculated total AUC value was 8516.56 and this means prediction accuracy of 85.17 % as result of verification.

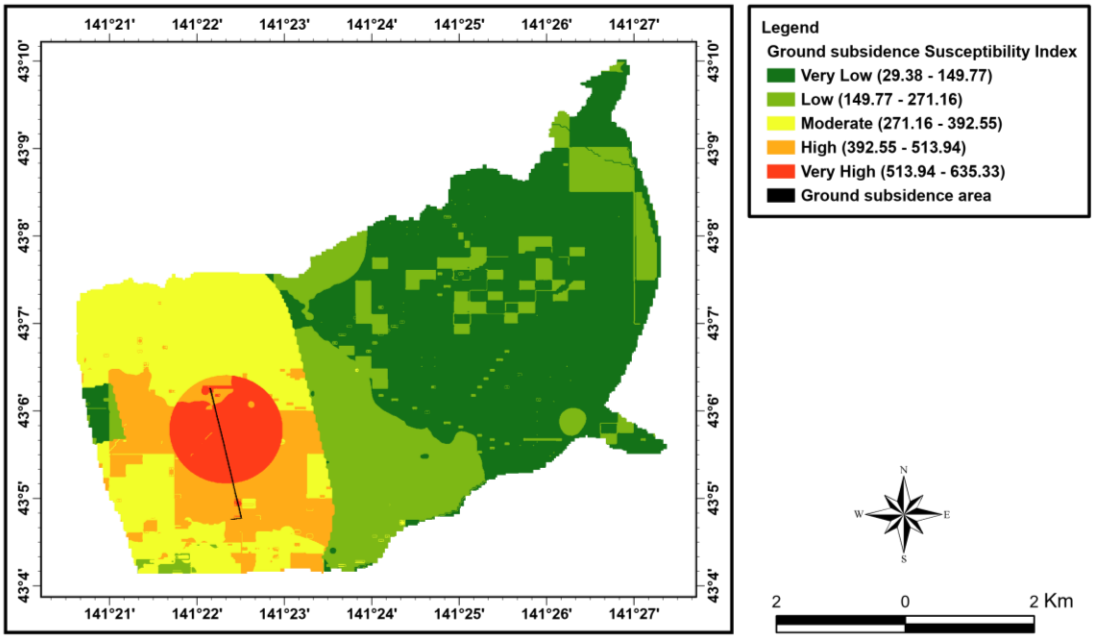

Figure 17. Earthquake-induced ground subsidence susceptibility map for Higashi Ward.

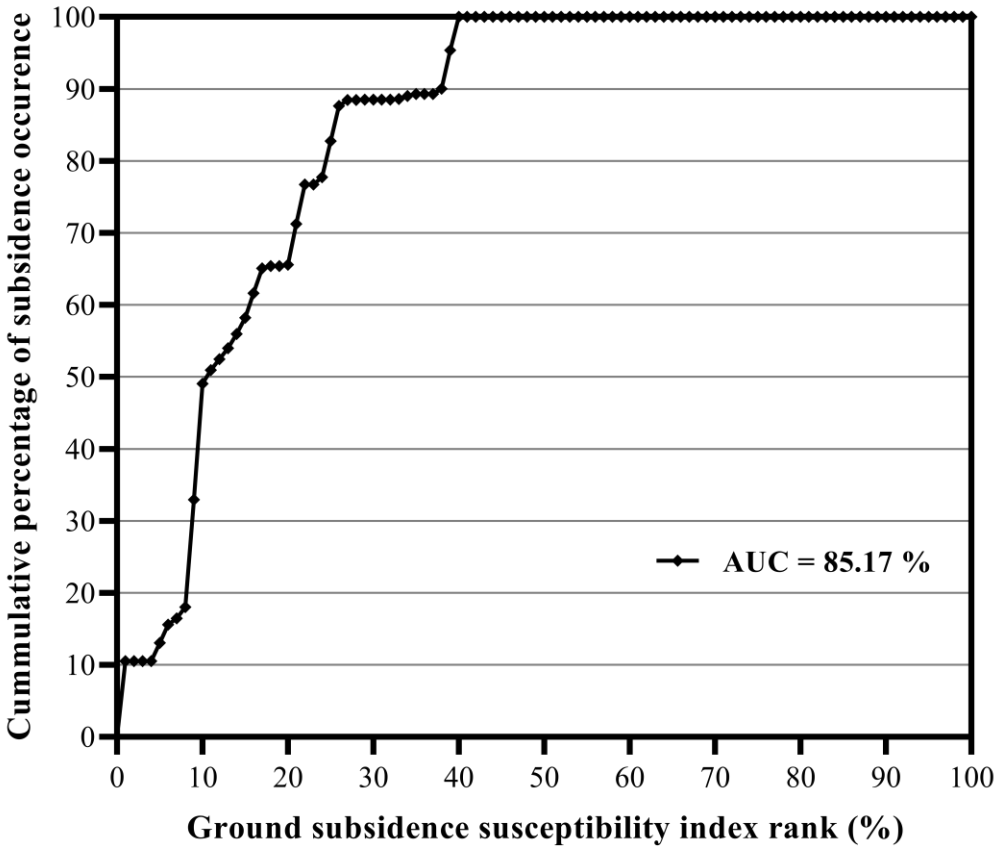

Figure 18. Verification result and accuracy of constructed EGSSM for Higashi Ward.

4.2 Analysis results of ground subsidence susceptibility in Kiyota Ward

4.2.1 Probability of ground subsidence

FR values of all seven factors including geology, slope, land use, ground water level, distance from railroad, precipitation and MMI are given in Table 6. These FR values are show how much the classes of each factor have influenced on earthquake-induced ground subsidence occurrence in the study area.

For geology, only the class of diluvial gravel had high FR values of 2.31 that indicates high probability of ground subsidence. Other classes had FR values of 0 and this means there is no possibility of subsidence.

In the case of slope, highest FR value was 2.21 at lowest degree from 0.2 to 3.27. And also, showed high probability of subsidence at low degree from 3.27 to 6.34 with FR value of 1.69. This result denotes that high probability of ground subsidence at areas with low slope angle in study area.

Factor of land use was divided into 8 subclasses including building site, forest, farm land, etc. land, lake, golf course, road and waste land. At the classes of etc. land and road had FR values of 1.17 and 1.90 respectively. Highest FR value of 3.40 was shown at the class of building site. This indicates very high probability of ground subsidence in this area and this is may be due to the characteristics of building site in study area. The building site is composed with residential area and constructed on the hilly area using cut and fill method. And volcanic ash soil was used as fillings but this soil is vulnerable to liquefaction during the earthquake shaking. As a result, this leads to high probability on ground subsidence, especially in the residential area.

For ground water level, probability was high at the range of 60.02-65.47 m and 65.57-72.84 m with FR value of 2.01 and 3.39, respectively. And showed slightly prone to ground subsidence at 43.15 to 50.51 m with ratio of 1.11.

In the case of distance from railroad, since there are no railroads in the study area, it was considered from the railroad data in other nearby wards in Sapporo. Peak FR value of 5.48 was showed at 3 to 5 km. From 1 to 3 km had FR value of 0.31 which indicates having very low probability of ground subsidence.

Subsidence probability for precipitation had highest FR value of 2.62 at the range of 9,808 to 10,226 mm and found no likelihood of ground subsidence at other classes.

For MMI, subsidence probability was increased as the intensity goes higher. Peak FR value of 3.47 was found at class of 7.5 to 8.0. This result indicates that areas where influence by strong intensity of earthquake are prone to ground subsidence.

Table 6. FR values for all classes of each factor for Kiyota Ward.

Factor	Classes	Class pixels (%)	Subsidence pixels (%)	FR
Geology	Diluvial gravel	43.37	100.00	2.31
	Sandstone, mudstone, gravel stone	30.09	0.00	0.00
	Volcanic ash loam	21.96	0.00	0.00
	Gravel and clay	4.58	0.00	0.00
Slope (Degree)	0.2-3.27	28.64	63.27	2.21
	3.27-6.34	21.76	36.73	1.69
	6.34-9.99	29.17	0.00	0.00
	9.99-14.18	14.90	0.00	0.00
	14.18-22.90	5.53	0.00	0.00
Land use	Building site	25.83	87.76	3.40
	Forest	59.56	1.02	0.02
	Farm land	2.39	0.00	0.00
	Etc. land	6.09	7.14	1.17
	Lake	0.95	0.00	0.00
	Golf course	2.45	0.00	0.00
	Road	2.15	4.08	1.90
	Waste land	0.58	0.00	0.00
Ground water level (m)	19.79-33.21	2.35	0.00	0.00
	33.21-43.15	4.81	1.02	0.21
	43.15-50.51	6.44	7.14	1.11
	50.51-55.97	21.23	13.27	0.62
	55.97-60.02	37.19	4.08	0.11
	60.02-65.47	14.73	29.59	2.01
	65.47-72.84	13.25	44.90	3.39

Table 6. (continued)

Factor	Classes	Class pixels (%)	Subsidence pixels (%)	FR
Distance from railroad (Km)	0-1	2.11	0.00	0.00
	1-3	16.26	5.10	0.31
	3-5	17.31	94.90	5.48
	5-7	17.22	0.00	0.00
	7-9	19.24	0.00	0.00
	9-12	0.00	0.00	0.00
	12-15	0.00	0.00	0.00
Precipitation (mm)	9,808-10,226	38.13	100.00	2.62
	10,226-10,874	5.46	0.00	0.00
	10,874-11,457	12.07	0.00	0.00
	11,457-12,474	31.41	0.00	0.00
	12,474-14,224	12.94	0.00	0.00
MMI	6.4-7.0	38.69	0.00	0.00
	7.0-7.5	34.24	6.12	0.18
	7.5-8.0	27.08	93.88	3.47

4.2.2 Interrelationship between factors and ground subsidence

From the results of FR values for all classes of each factor, RF value was prepared for normalization from 0 to 1. Then, to identify the major ground subsidence trigger factors, PR was calculated using frequency ratio model. PR values denote weights of each ground subsidence conditioning factor and calculated PR values are presented in Figure 19. Results showed that precipitation and geology were most influential factors on ground subsidence among the 7 subsidence conditioning factors. MMI was second most influential factor and distance from railroad had also high contribution to ground subsidence occurrence with PR value of 2.08. Relatively, factor of ground water level, land use and slope have low influence in this study area.

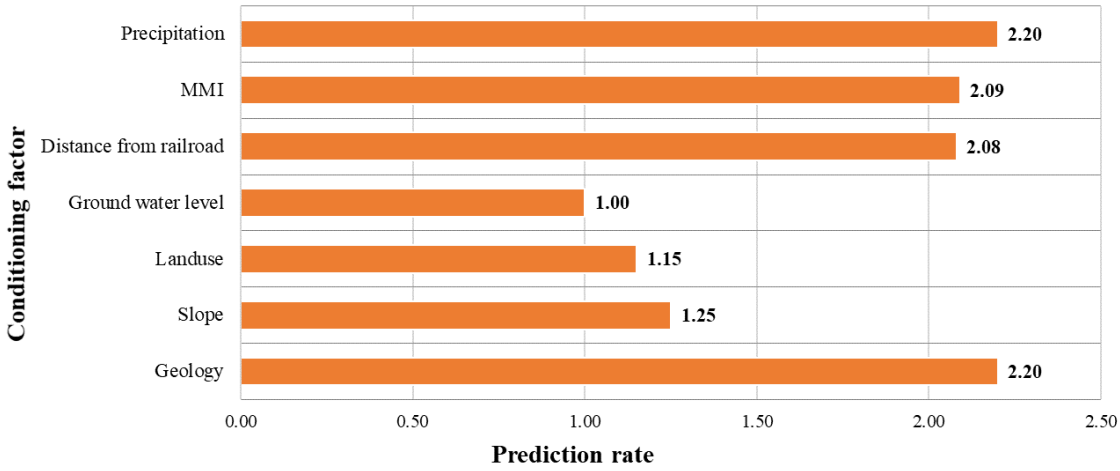

Figure 19. PR values for all ground subsidence conditioning factors in Kiyota Ward.

4.2.3 Overlay analysis between conditioning factors

Before construct the final hazard map, to identify how each factor would affect the final outcome, overlay analysis was performed with 6 subsidence trigger factors except ground water level that having lowest weight on ground subsidence. For this purpose, 3 overlaid maps were constructed between factor of (1) land use and slope, (2) MMI and distance from railroad and (3) precipitation and geology, respectively (Figure 20-22). Figure 20 presenting the result of overlaid layer of land use and slope and calculated GSSI value was from 0 to 129.80. Highly prone to ground subsidence areas were found in residential areas with low hill or plain areas. This is because the residential area was constructed after cutting the hilly areas and filling with volcanic ash soil as mentioned in the results of FR values. This indicates residential site of the study area is very vulnerable to ground subsidence that influenced by earthquake.

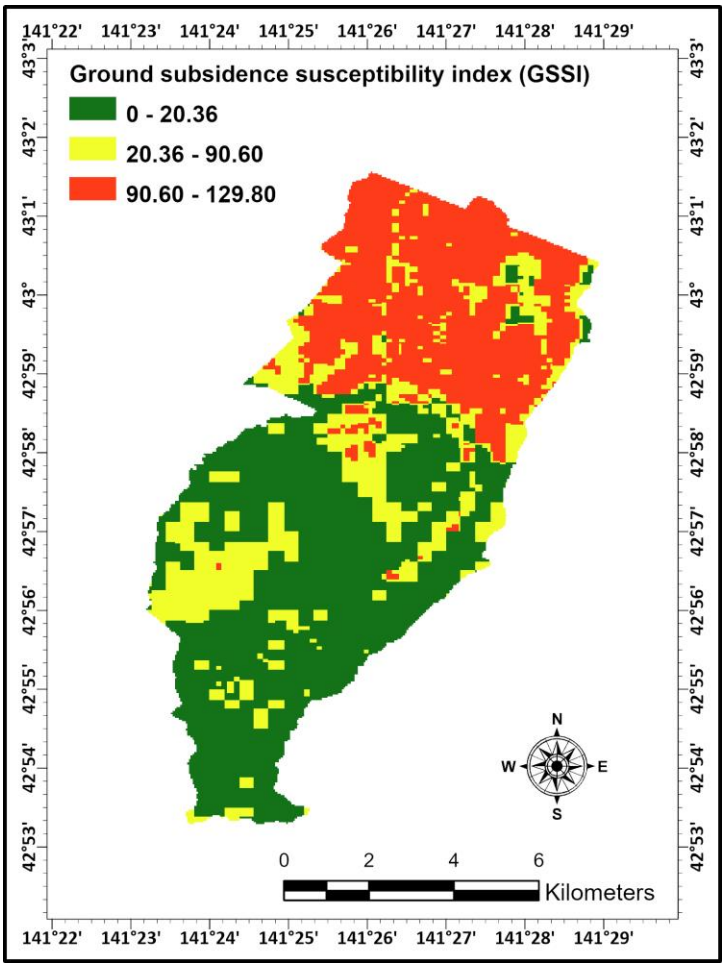

Figure 20. Result of overlay analysis between factor of land use and slope.

Result of calculated GSSI values between factor of MMI and distance from railroad had from 0 to 394.07 as shown in Figure 21. High GSSI values from 208.62 to 394.07 were showed at the areas where influenced by high intensity of earthquake (7.5 - 8.0) and close to the railroads (1 - 5 km). This result denotes that risk of ground subsidence is high under the condition of MMI over 7.5 and areas located within 5 km from railroads in the study area. Also, this result had highly influence to the mapping of EGSSM.

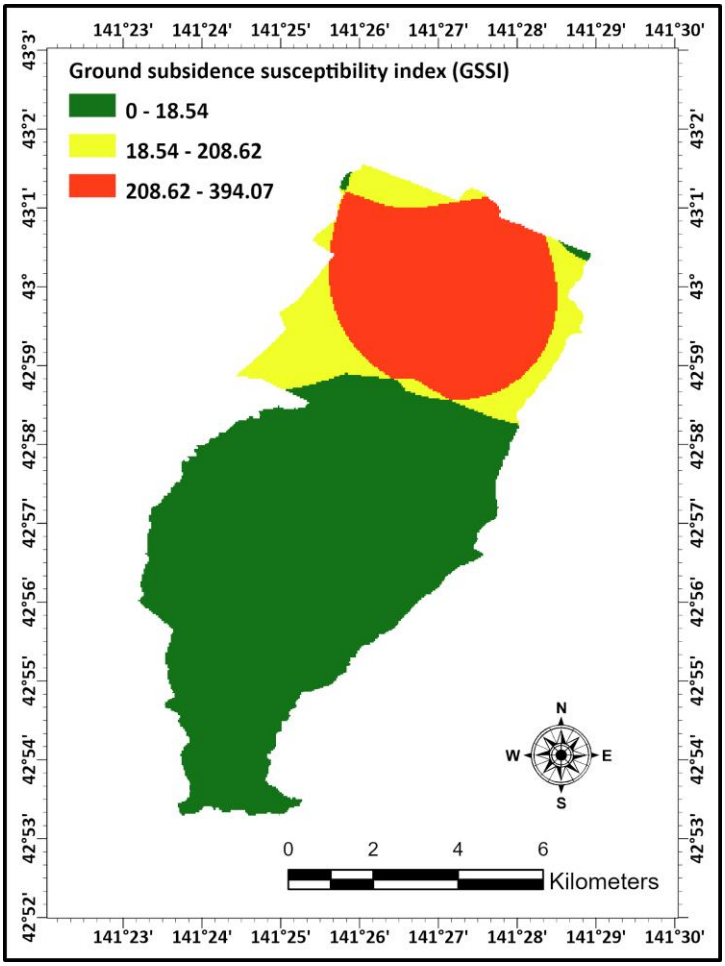

Figure 21. Result of overlay analysis between factor of MMI and distance from railroad.

Factor of precipitation and geology were had highest weight among all ground subsidence conditioning factors. And this indicates these two factors had the greatest impact on the ground subsidence occurrence in this study. GSSI value was also very high having maximum 440 against results of 2 other overlaid layer (Figure 22). High index values were found in areas composed with diluvial gravel and had lowest total amount of

precipitation. Probability of prone to ground subsidence was high at the range of lowest total amount of rainfall during the past 30 years, but this can be explained as because there was intensive rainfall when the 2018 Hokkaido eastern Iburi earthquake have occurred.

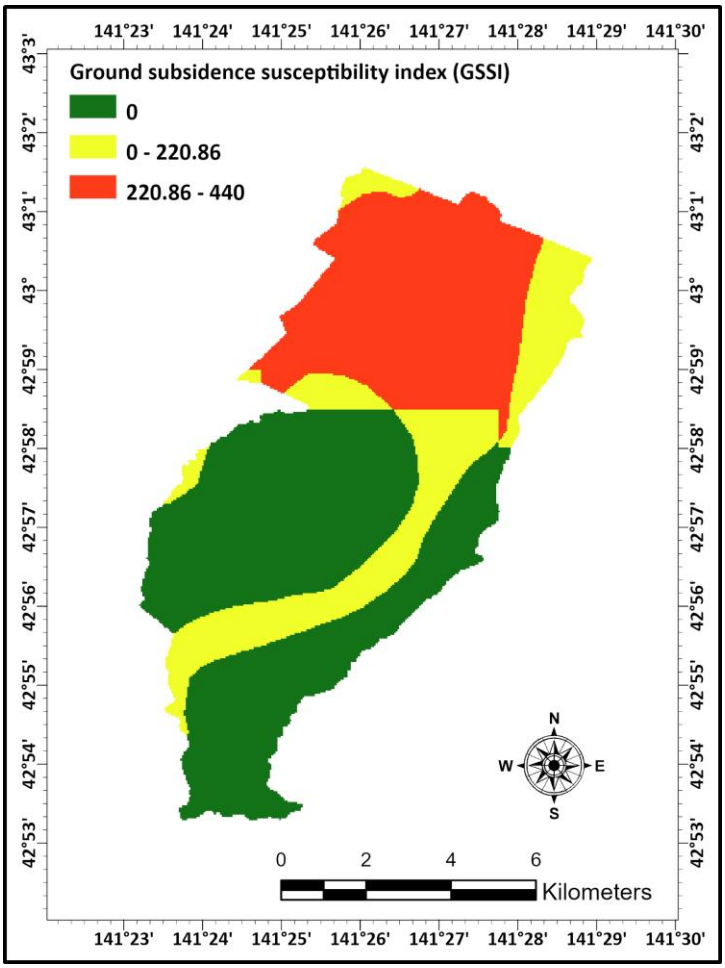

Figure 22. Result of overlay analysis between factor of precipitation and geology.

4.2.4 Susceptibility map and validation

From the prepared RF and PR values of all factors, GSSI was calculated by using Equation (3) and EGSSM was constructed as shown in Figure 23. GSSI of predicted EGSSM was ranged from 1 to 1008.87 in this study. For better identification, GSSI was reclassified by dividing into 5 levels including very low (1-143.29), low (143.29-396.24), moderate (396.24-653.15), high (653.15-862.13) and very high (862.63-1008.87). In the study area, total 98 points of actual ground subsidence have occurred. Against the final hazards map, it was found that all of ground subsidence have occurred in areas having high and very high ground subsidence susceptibility. Total 88.78% of ground subsidence have occurred in very high-level areas of GSSI and 11.22% have occurred in high level areas (Table 7).

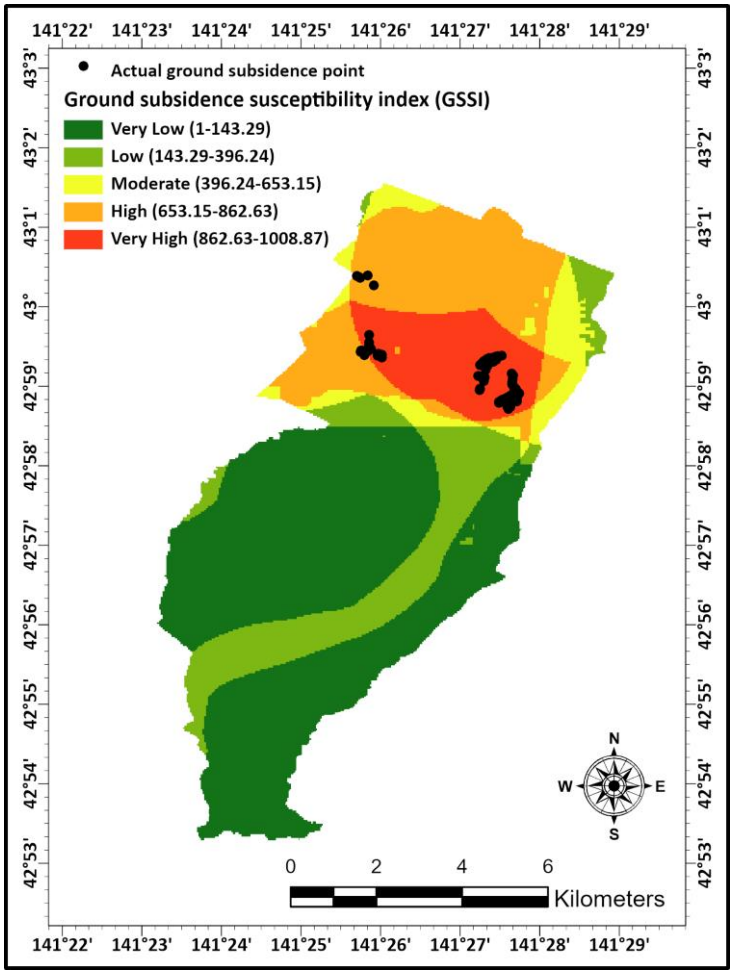

Figure 23. Earthquake-induced ground subsidence susceptibility map for Kiyota Ward.

Table 7. Subsidence points percentage for GSSI level of predicted EGSSM.

GSSI level	Number of Subsidence point	Subsidence percentage (%)
Very low	0 / 98	0
Low	0 / 98	0
Moderate	0 / 98	0
High	11 / 98	11.22
Very high	87 / 98	88.78

In this study, area under curve (AUC) was applied for the vilification of the predicted EGSSM for study area. Prediction accuracy of EGSSM was evaluated by comparing with actual ground subsidence area as stated above and result is shown in Figure 24. Verification result showed that, 89% of all ground subsidence have occurred in 10% of study area having high ground subsidence susceptibility index level. Also, in 25 % of study area, occurred 95 % of all ground subsidence and all of ground subsidence has occurred in 32 % of study area. Calculated total AUC value was 9614.286 and this denotes that 96.14% of prediction accuracy of constructed EGSSM.

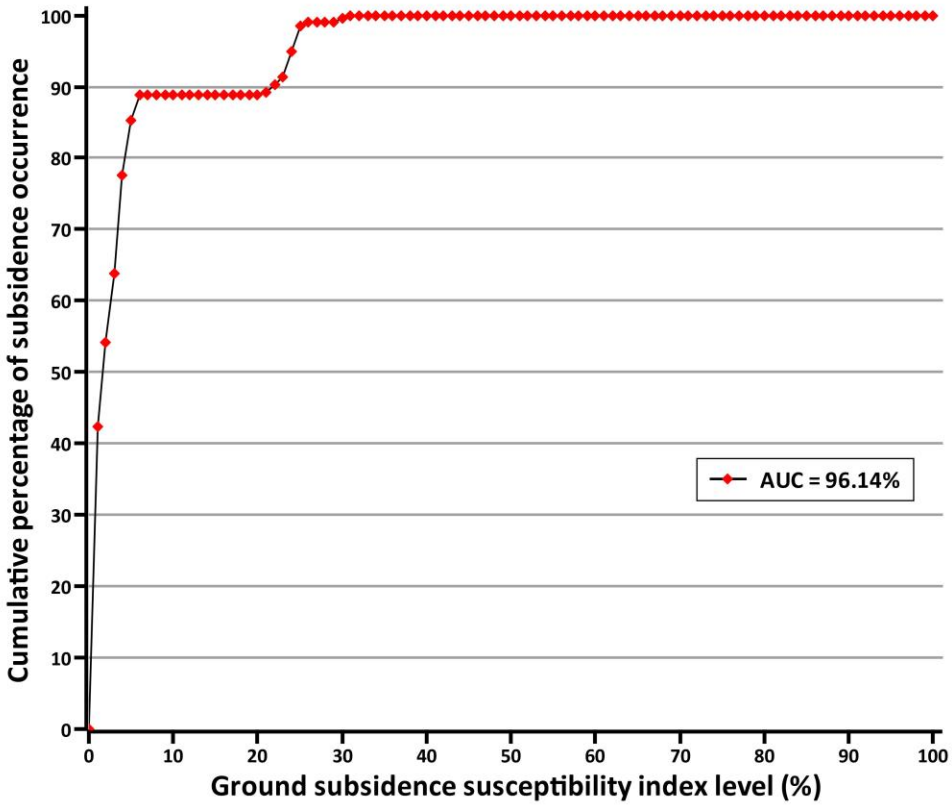

Figure 24. Verification result and accuracy of constructed EGSSM for Kiyota Ward.

4.3 Analysis results of ground subsidence susceptibility in Sapporo

4.3.1 Probability of ground subsidence

To identify the relationship between ground subsidence and 7 ground subsidence conditioning factors, FR values were calculated using frequency ratio model. Table 8 shows calculation results of chosen 7 factors as follows: geology, slope (degree), land use, ground water level, distance from railroad and subway line, precipitation and MMI. These results indicate how much the classes of each factor have influenced on earthquake-induced ground subsidence occurrence in the study area.

Factor of geology was divided into 5 classes include andesite, volcanic gravel, gravel and clay, sandstone, mudstone and gravel and volcanic ash and loam. In the relationship between ground subsidence and geology, classes of volcanic gravel had highest FR value of 6.35 that means having high probability of ground subsidence. And showed slightly prone to ground subsidence at the class of gravel and clay as FR value of 1.79.

Slope angle sub-classified to 5 classes as degree range from 1 to 40.7. Peak FR value was 1.64 at lowest degree from 1 to 4.6. And showed FR values over than 1 at the degree of 18.3 to 25. From this result, it was founded that there was no particular correlation between ground subsidence and steepness of the slope angle in this study area.

Table 8. FR values of seven ground subsidence conditioning factors for Sapporo.

Factor	Classes	Class pixels (%)	Subsidence pixels (%)	FR
Geology	Andesite	25.60	0.00	0.00
	Volcanic gravel	7.96	50.52	6.35
	Gravel and clay	27.69	49.48	1.79
	Sandstone, mudstone, gravel	36.41	0.00	0.00
	Volcanic ash and loam	2.35	0.00	0.00
Slope (Degree)	1-4.6	37.72	61.86	1.64
	4.6-11.6	20.88	5.15	0.25
	11.6-18.3	19.51	9.28	0.48
	18.3-25	16.27	23.71	1.46
	25-40.7	5.62	0.00	0.00
Land use	Forest	66.64	0.52	0.01
	Lake	2.18	0.00	0.00
	Etc. Land	4.70	0.52	0.11
	Building site	18.73	84.54	4.51
	Waste land	2.73	0.00	0.00
	Golf course	0.48	0.00	0.00
	Farm land	2.79	0.00	0.00
	Road	1.44	14.43	10.00
	Rice paddy	0.05	0.00	0.00
	Railroad	0.26	0.00	0.00

Table 8. (continued)

Factor	Classes	Class pixels (%)	Subsidence pixels (%)	FR
Ground water level (m)	0-35.20	32.05	100.00	3.12
	35.20-59.05	31.58	0.00	0.00
	59.05-95.33	28.69	0.00	0.00
	95.33-150.53	6.51	0.00	0.00
	150.53-234.53	0.69	0.00	0.00
	234.53-362.34	0.30	0.00	0.00
	362.34-556.81	0.18	0.00	
Distance from railroad and subway line (Km)	0-1	16.12	49.48	3.07
	1-5	34.29	50.52	1.47
	5-10	27.24	0.00	0.00
	10-15	15.40	0.00	0.00
	15-20	6.91	0.00	0.00
	20-25	0.00	0.00	0.00

Table 8. (continued)

Factor	Classes	Class pixels (%)	Subsidence pixels (%)	FR
Precipitation (mm)	9,448-10,735	26.00	100.00	3.85
	10,735-12,186	8.99	0.00	0.00
	12,186-13,318	23.09	0.00	0.00
	13,318-14,312	27.83	0.00	0.00
	14,312-15,513	13.24	0.00	0.00
	15,513-18,153	0.84	0.00	0.00
MMI	5.00-5.81	5.84	0.00	0.00
	5.81-6.34	33.12	0.00	0.00
	6.34-6.81	31.08	0.00	0.00
	6.81-7.36	19.55	48.45	2.48
	7.36-8.02	10.05	18.56	1.85
	8.02-9.00	0.35	32.99	94.55

In the case of land use, it was sub-classified to 10 classes as below: forest, lake, etc. land, building site, waste land, golf course, farm land, road, rice paddy and railroad. Highest FR value of 10 was shown at the class of road. And also, showed high probability to ground subsidence at building site as FR value of 4.51. These results denote that where on or in around roads and building sites are highly prone to ground subsidence.

Factor of ground water level was categorized into 7 classes in scope of 0 to 556.81 m. Result showed only had high FR values as 3.12 at the range of 0 to 35.2 m. Other classes had FR values of 0 and this means very low possibility of subsidence.

Distance from railroad and subway line was reclassified into 6 classes, ranging from 0 to 25 Km at intervals of 5 Km except first subclass (0 to 1 Km). About relationship between ground subsidence and distance from railroad and subway line, probability of ground subsidence was high from range of 0 to 10 Km. And peak FR value was 3.07 at the class of 0 to 1 Km. This indicates, where located closer to the railroad and subway line is more prone to ground subsidence.

In the case of precipitation, total amount of rainfall in past 30 years was considered and categorized into 6 classes in range of 9,448 to 18,153 mm. Highest FR value of 3.85 was founded at class of least total amount of rainfall that range of 9,448 to 10,735 mm and there was no likelihood of ground subsidence at other classes.

Intensity of earthquake was divided into 6 classes as below: 5.00-5.81, 5.81-6.34, 6.34-6.81, 6.81-7.36, 7.36-8.02, 8.02-9.00. Subsidence probability was high from the range of 6.81 to 9.00. Highest FR value was 94.55 at the class of highest intensity range

(8.02-9.00). This result denotes where influenced by high intensity of earthquake is more prone to ground subsidence.

4.3.2 Interrelationship between factors and ground subsidence

From the analysis results of correlation between ground subsidence occurrence and 7 selected conditioning factors, RF values were calculated to normalize the FR values as range of 0 to 1. Then, PR values were derived from RF for individual weightage of all considered 7 parameters in this study. PR values were utilized to calculation of GSSI and construction of EGSSM. Calculated PR values of 7 conditioning factors are presented in Figure 25. Results showed that factors of ground water level and precipitation were most influential factors on ground subsidence among the 7 subsidence conditioning factors. Also, MMI had high correlation with ground subsidence occurrence as PR values of 2.23. Geology, land use and railroad and subway line had some contribution to ground subsidence occurrence. Relatively, slope angle had low influence on ground subsidence in this study area.

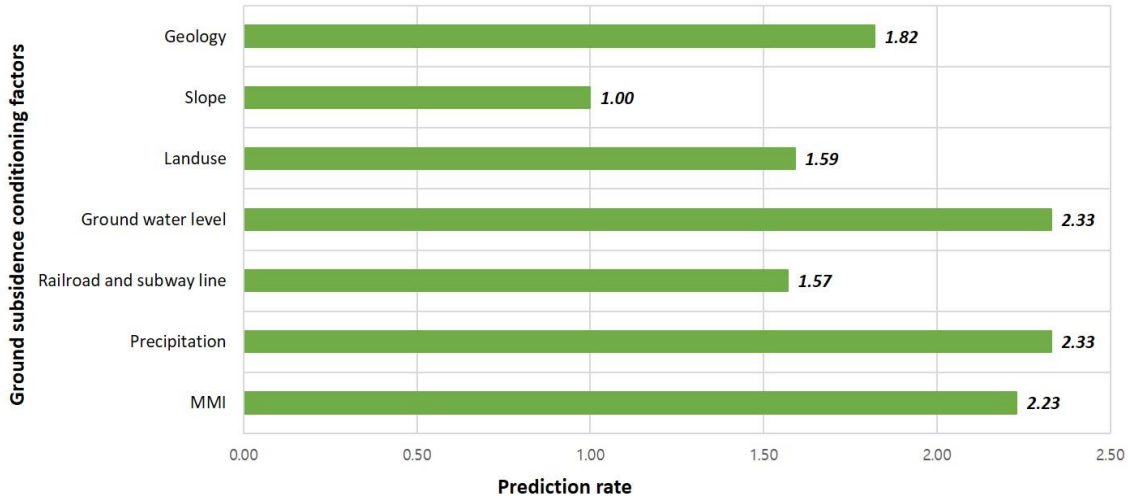

Figure 25. PR values for all ground subsidence conditioning factors in Sapporo.

4.3.3 Overlay analysis between conditioning factors

From these results, overlay analysis was conducted with 6 ground subsidence causative factors to determine how each factor affects to EGSSM of study area. Analysis was performed except slope angle which had lowest influence on ground subsidence. For this purpose, 3 overlaid thematic maps were constructed between factor of (1) land use and distance from railroad and subway line, (2) geology and MMI, (3) ground water level and precipitation, respectively (Figure 26-28).

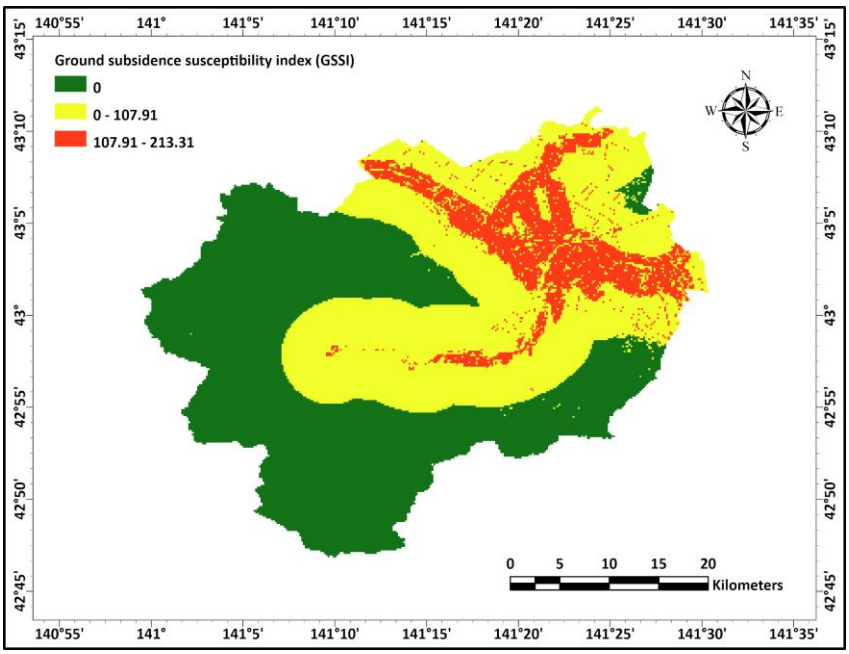

Figure 26. Result of overlay analysis between factor of land use and railroad and subway line.

The overlay analysis result between factor of land use and distance from railroad and subway line is given in Figure 26. Calculated GSSI value was from 0 to 213.31 and higher GSSI value means more vulnerable to ground subsidence. From this overlaid layer, it was founded that building sites, roads and areas located to near the railroad subway line was highly susceptible to ground subsidence in this study. This indicates that areas consist with a large number of buildings including apartments, stores and other infrastructures had high potential risk of ground subsidence. And also, including roads, especially constructed on the underground structures such as subway lines.

Figure 27 shows overlaid thematic map between geology and MMI. Result of calculated GSSI values had from 0 to 250.07. High GSSI values (42.17 to 250.07) were

founded at the areas composed with volcanic gravel, gravel and clay and influenced by strong MMI over than 6.34 (6.34 to 9.00). This result denotes that under condition of strong shaking by earthquake as intensity over 6.34, the ground composed with above soil types in the study area is prone to soil liquefaction phenomena and it leads to hazard of ground subsidence.

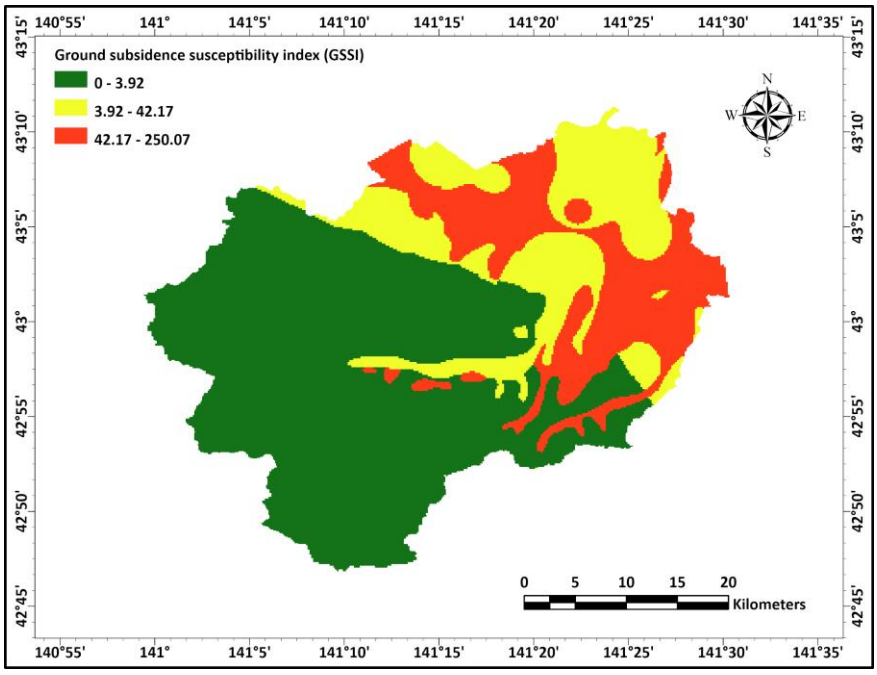

Figure 27. Result of overlay analysis between factor of geology and MMI.

Ground water level and precipitation had highest influence on the ground subsidence in this study. Figure 28 shows the analysis result of overlaid these two factors and GSSI value was from 0 to 466. Peak GSSI value was 466 and this means highest probability of ground subsidence among the results of 3 overlaid layers. High index values were identified in areas had lowest ground water level as range of 0 to 35.20 m

and least total amount of precipitation (9,448 to 10,735). When the 2018 Hokkaido eastern Iburi earthquake has occurred, there was intensive rainfall in Sapporo regions. Hence, despite the overlaid map showed very high vulnerability of ground subsidence at areas with least total amount of precipitation, it could be explained that there was ground deformation as the underground water level increased as a result of affected by this heavy rain.

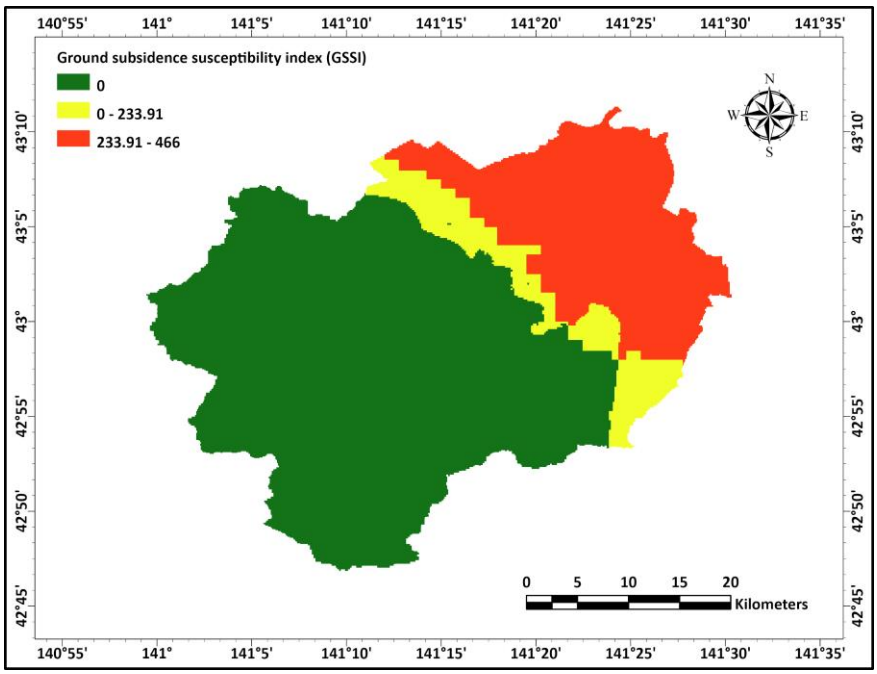

Figure 28. Result of overlay analysis between factor of ground water level and precipitation.

4.3.4 Susceptibility map and validation

By combining calculated PR values of each factor and RF values of each class, GSSI was calculated for study area and EGSSM was constructed as given in Figure 29. Predicted EGSSM had GSSI values range of 0 to 971.38 in this study. And the GSSI values were reclassified to 5 subclasses as below: very low (0-114.28), low (114.28-304.75), moderate (304.75-518.07), high (518.07-670.44) and very high (670.44-971.38). Investigated total ground subsidence points in the study area were 194 and 96 points had occurred in Higashi-Ward and 98 points had occurred in Kiyota-Ward of Sapporo. From the constructed EGSSM, it was identified that all of ground subsidence points have occurred in regions with very high vulnerability index.

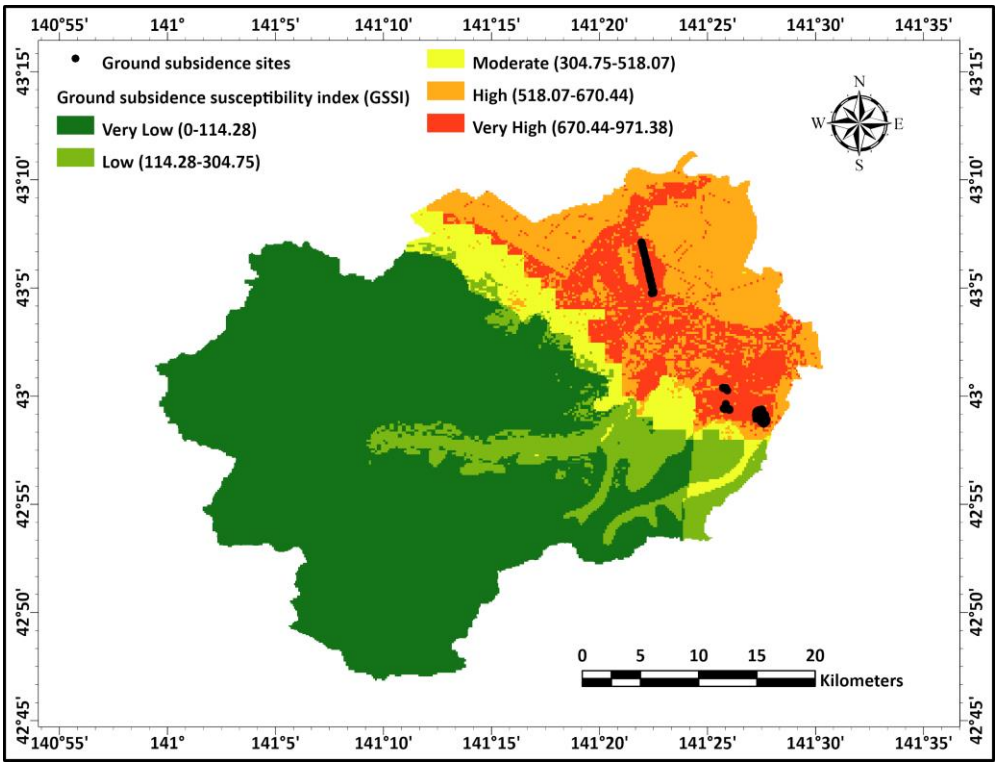

Figure 29. Earthquake-induced ground subsidence susceptibility map for Sapporo.

For the verification, predicted EGSSM was compared with investigated and prepared ground subsidence inventory. For this purpose, area under curve (AUC) was applied in this study and results are given in Figure 30. Verification result showed that, 33.3 % of all ground subsidence have occurred in 10 % of study area having high ground subsidence susceptibility index level. Also, in 25 % of study area, occurred 70 % of all ground subsidence and all of ground subsidence has occurred in 29 % of study area. Calculated total AUC value was 8321.67 and this means 83.22 % of prediction accuracy of predicted EGSSM for Sapporo.

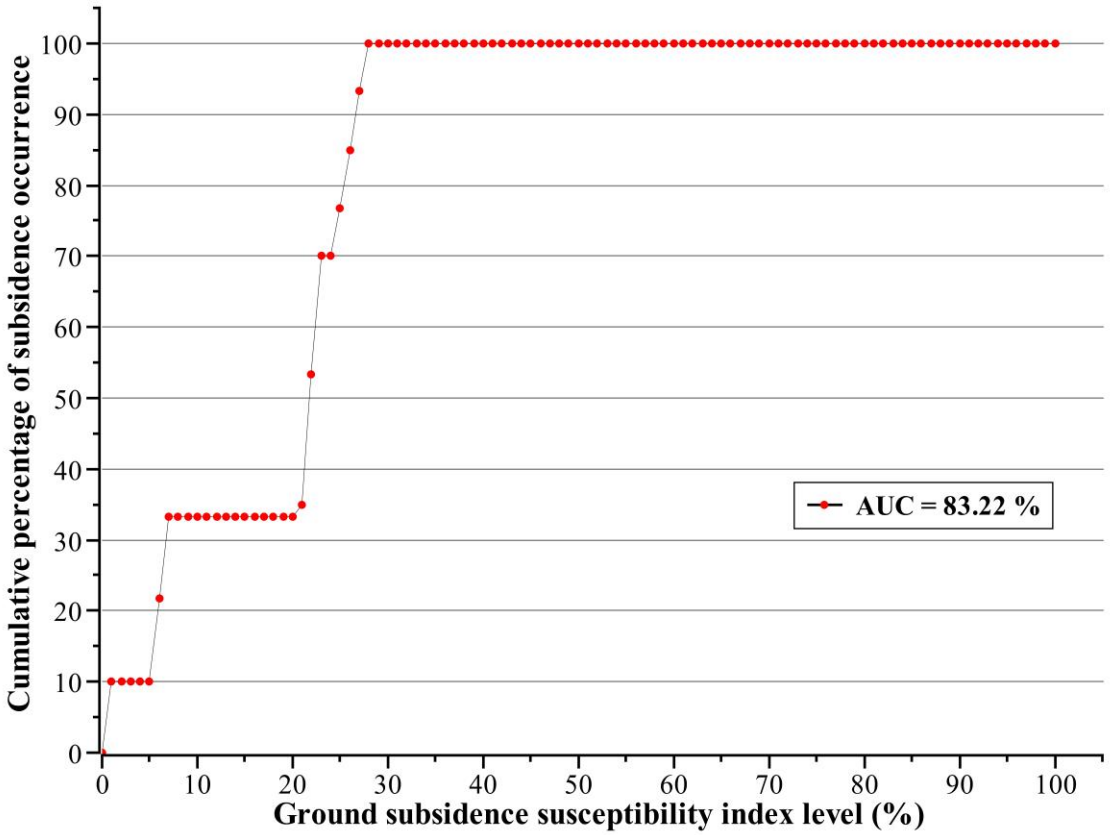

Figure 30. Verification result and accuracy of constructed EGSSM for Sapporo.

Chapter V

Conclusion and Recommendation

5.1 Conclusion

Disastrous damages are increasing in urban areas worldwide from the hazards of ground subsidence. Also, in many countries including Japan, a number of ground subsidence have occurred by earthquakes which is one of the major subsidence triggers. Restoration work has been carried out as a countermeasure after the damage but it costs high and also having difficulties on complete restore, especially in urban areas. Moreover, in previous studies, assessment of earthquake-induced ground subsidence in urban areas has not been well studied. For the risk prevention and efficient hazard reduction, assessment of susceptibility on this multi-hazard is highly needed. Therefore, the aim of this study was predicting and mapping vulnerability on the risk of earthquake-induced ground subsidence in the Higashi, Kiyota ward and Sapporo, Japan. In this article, statistical analysis method (Frequency ratio model) and GIS technique (ArcGIS Pro) were applied for this purpose. The achievements and contributions of this study is as follows:

1. Past ground subsidence location map was prepared from the investigated information in final report of 2018 Hokkaido Eastern Iburi earthquake performed by Japanese Geotechnical Society. Location map for the Higashi ward was prepared as polygon data. Other maps for Kiyota ward and Sapporo were prepared as points data with 98 and 194 subsidence location points, respectively.

2. Seven ground subsidence conditioning factors including geology (lithology), slope angle, land use, ground water level, distance from railroad and subway line, precipitation and intensity of earthquake (MMI) were considered and constructed as thematic layers. All factors were selected after literature review of past researches on ground subsidence for the accurate analysis results.

3. Correlation between earthquake-induced ground subsidence and considered seven conditioning factors were identified using frequency ratio model. Results showed that factor of distance from railroad and subway line has highest influence to ground subsidence with weight of 2.12 in Higashi ward. In the case of Kiyota ward, factor of geology and precipitation were most influential factors on subsidence with weight of 2.2. For Sapporo, factors of ground water level and precipitation had highest influence to the earthquake-induced ground subsidence, as weight of 2.33. Also, factor of MMI was one of the major trigger factors as weight of 2.23.

4. Produced earthquake-induced ground subsidence susceptibility map (EGSSM) for each Higashi, Kiyota ward and Sapporo using weights of each factors and ground subsidence susceptibility index (GSSI). For easier understanding, vulnerability of ground subsidence was reclassified and expressed into 5 classes: very low, low, moderate, high and very high. Ground subsidence vulnerability was very high on the subway lines in Higashi ward and residential areas in Kiyota ward. High vulnerability areas of ground subsidence in Sapporo were widely distributed over

multiple administrative districts except Minami-Ward. However, specifically, very high subsidence vulnerability level areas were showed at railroads, subway lines and building sites including residential areas.

5. Performance of hazard mapping system was assessed by area under curve (AUC) approach by comparing results of prepared past ground subsidence location map and constructed EGSSM. Verification results showed prediction accuracy of 83.22% for Higashi ward, 96.14% for Kiyota ward and 83.22% for entire area of Sapporo.

The findings of present study have showed major ground subsidence causative factors on earthquake-induced ground subsidence in Sapporo and also, produced EGSSM with reliable prediction accuracy. These results could be helpful to the disaster risk reduction and management in urban areas. Moreover, by providing information of weakness location on ground subsidence for the specific areas, EGSSM can be used as an efficient material for the city planners and engineers for making appropriate decision on development or reinforcement plans.

5.2 Recommendation

This study made new attempt on the assessment of the earthquake-induced ground subsidence in Sapporo and produced reliable hazard map. However, there were several defects in aspects of data collection, data analysis, applicated model and verification. Problems detected in the current study are as follows:

1. Data collection: In general, when perform the geospatial analysis as well as hazards assessment, original data sources can be obtained from reliable agencies and organ of government. In this regard, it is highly needed the cooperation of maintaining and providing recent information through possible continuous scrutiny for the reliable and accurate analysis. For instance, the status of land use due to accelerating development in urban areas is likely to change over time.

2. Data analysis: In the case of factor of ground water level, the layer was prepared using Inverse distance weighting (IDW) interpolation method was used with borehole databases. However, in the case of study area of Sapporo is nearly half of the area consists of mountainous areas and borehole data was couldn’t obtained and used for this area. Result of IDW analysis without borehole databases of the area be relatively inaccurate. Thus, more careful consideration is needed about this point in the future works.

3. Analysis model: In this study, only one statistical model (frequency ratio model) was applicated for the hazard assessment based on GIS technique. Frequency ratio

model is widely used from past to present and showed good performance on the research of various hazards assessment. However, in many of current studies proposed model application of various quantitative analysis models such as artificial neural networks for the comparison. Thus, more progressed model should be applicated for the future work to improve the performance.

4. Verification: Applicated AUC method for the verification of constructed hazard map could be insufficient to provide a convincing assessment of the model. To overcome this shortcoming, the model should be validated by using a second dataset. Thus, in future work, data of ground subsidence location should be divided into two datasets and be used for the model testing and verification, respectively.

References

Abdollahi S., Pourghasemi H. S., Ghanbarian G. A., Safaeian, R. 2019. Prioritization of effective factors in the occurrence of land subsidence and its susceptibility mapping using an SVM model and their different kernel functions. Bulletin of Engineering Geology and the Environment 78, 4017-4034.

Abidin H. Z., Andreas H., Gumilar I., Sidiq T. P., & Gamal M. 2015. Environmental impacts of land subsidence in urban areas of Indonesia. In FIG Working Week, 1-12.

Acharya T. D. and Lee D. H. 2019. Landslide Susceptibility Mapping using Relative Frequency and Predictor Rate along Araniko Highway. KSCE Journal of Civil Engineering 23(2), 763-776.

Aimaiti Y., Liu W., Yamazaki F. & Maruyama Y. 2019. Earthquake-induced landslide mapping for the 2018 Hokkaido Eastern Iburi Earthquake Using PALSAR-2 data. Remote Sensing, 11(20), 2351.

Akgun A., Dag S. and Bulut F. 2007. Landslide susceptibility mapping for a landslide-prone area (Findikli, NE of Turkey) by likelihood-frequency ratio and weighted linear combination models. Environmental Geology 54, 1127-1143.

Arabameri A., Saha S., Roy J., Tiefenbacher J. P., Cerda A., Biggs T., Pradhan B., Thi Ngo P. H., Collins A. L. 2020. A novel ensemble computational intelligence approach for the spatial prediction of land subsidence susceptibility. Science of The Total Environment, 726, 138595.

Arabameri A., Pal S. C., Rezaie F., Chakrabortty R., Chowdhuri I., Blaschke T., Thao P. 2021. Comparison of multi-criteria and artificial intelligence models for land-

subsidence susceptibility zonation. Journal of Environmental Management 284, 112067.

Avilés-Campoverde D., Chunga K., Ortiz-Hernández E., Vivas-Espinoza E., Toulkeridis T., Morales-Delgado A., Delgado-Toala D. 2021. Seismically Induced Soil Liquefaction and Geological Conditions in the City of Jama due to the M7.8 Pedernales Earthquake in 2016, NW Ecuador. Geosciences 11(1), 20.

Bianchini S., Solari L., Soldato M. D., Raspini F., Montalti R., Ciampalini A. and Casagli N. 2019. Ground Subsidence Susceptibility (GSS) Mapping in Grosseto Plain (Tuscany, Italy) Based on Satellite InSAR Data Using Frequency Ratio and Fuzzy Logic. Remote Sensing 11(17), 2015.

Blasco JM. D., Foumelis M., Stewart C and Hooper A. 2019. Measuring Urban Subsidence in the Rome Metropolitan Area (Italy) with Sentinel-1 SNAP-StaMPS Persistent Scatterer Interferometry. Remote Sensing 11(2), 129.

Bradley A. P., 1997. The use of the area under the ROC curve in the evaluation of machine learning algorithms. Pattern Recognition, 30(7), 1145-1159.

Bui D. T., Shahabi H., Shirzadi A., Chapi K., Pradhan B., Chen W., Khosravi K., Panahi M., Ahmad B. B. and Lee S. 2018. Land Subsidence Susceptibility Mapping in South Korea Using Machine Learning Algorithms. Sensors 18(8), 2464.

Cao C., Xu P., Wang Y., Chen J., Zheng L and Niu C. 2016. Flash Flood Hazard Susceptibility Mapping Using Frequency Ratio and Statistical Index Methods in Coalmine Subsidence Areas. Sustainability 8(9), 948.

Choi J. K., Kim K. D., Lee S., Kim I. S., Won J. S. 2007. Prediction of Ground Subsidence Hazard Area Using GIS and Probability Model near Abandoned Underground Coal Mine. Econ. Environ. Geol 40(3), 295-306.

Choi J. K., Kim K. D., Lee S., Won J. S. 2010. Application of a fuzzy operator to susceptibility estimations of coal mine subsidence in Taebaek City, Korea. Environ Earth Sci 59: 1009-1022.

Cotecchia V. 1986. Subsidence phenomena due to earthquakes: Italian cases. IAHS-AISH publication 151, 829-8340.

Dai F. C., Lee C. F., Li J., Xu Z. W. 2001. Assessment of landslide susceptibility on the natural terrain of Lantau Island, Hong Kong. Environmental Geology 40(3), 381-391.

Ding Q., Chen W and Hong H. 2017. Application of frequency ratio, weights of evidence and evidential belief function models in landslide susceptibility mapping. Geocarto International 32(6), 619-639.

Ezquerro P., Albert C., Herrera G., Merodo A., Pizarro M. and Boni R. 2017. Groundwater and Subsidence Modeling Combining Geological and Multi-Satellite SAR Data over the Alto Guadalentín Aquifer (SE Spain). Geofluids vol. 2017.

Fujiwara S., Nakano T., Morishita Y. et al. 2019. Detection and interpretation of local surface deformation from the 2018 Hokkaido Eastern Iburi Earthquake using ALOS-2 SAR data. Earth Planets Space 71, 64.

Holzer T. L., Johnson A. I. 1985. Land subsidence caused by ground water withdrawal in urban areas. GeoJournal 11, 245-255.

Ilia I., Loupasakis C and Tsangaratos P. 2018. Land subsidence phenomena investigated by spatiotemporal analysis of groundwater resources, remote sensing techniques, and random forest method: the case of Western Thessaly, Greece. Environ Monit Assess 190, 623.

Intarawichian N., Dasananda S. 2011. Frequency ratio model based landslide susceptibility mapping in lower Mae Chaem watershed, Northern Thailand. Environ Earth Sci 64, 2271-2285.

Japanese Geotechnical Society. 2019. Final report of 2018 Hokkaido Eastern Iburi earthquake by the ground disaster investigation team. p. 70-90. https://www.jiban.or.jp/file/saigai/H30_Hokkaido_EQ_FinalReport.pdf

Japan Meteorological Agency. Retrieved from: https://www.jma.go.jp/jma/menu/menureport.html

Kaitantzian A., Loupasakis C., Tzampoglou P. and Parcharidis I. 2020. Ground Subsidence Triggered by the Overexploitation of Aquifers Affecting Urban Sites: The Case of Athens Coastal Zone along Faliro Bay (Greece). Geofluids, vol. 2020.

Karimzadeh S. and Matsuoka M. 2018. A Weighted Overlay Method for Liquefaction-Related Urban Damage Detection: A Case Study of the 6 September 2018 Hokkaido Eastern Iburi Earthquake, Japan. Geosciences 8(12):487.

Khan H., Shafique M., Khan M., Bacha M., Shah S., Calligaris C. 2019. Landslide susceptibility assessment using Frequency Ratio, a case study of northern Pakistan. The Egyptian Journal of Remote Sensing and Space Science. 22(1), 11-24.

Khorrami M., Abrishami S., Maghsoudi Y., Alizadeh B and Perssin D. 2020. Extreme subsidence in a populated city (Mashhad) detected by PSInSAR considering groundwater withdrawal and geotechnical properties. Scientific Reports 10, 11357.

Kim K. D., Lee S., Oh H. J., Choi J. K., Won J. S. 2006. Assessment of ground subsidence hazard near an abandoned underground coal mine using GIS. Environ Geol 50: 1183-1191.

Kim K. D., Lee S., Oh H. J. 2009. Prediction of ground subsidence in Samcheok City, Korea using artificial neural networks and GIS. Environ Geol 58: 61-70.

Lai C. G., Bozzoni F., Conca D. et al. 2020. Technical guidelines for the assessment of earthquake induced liquefaction hazard at urban scale. Bull Earthquake Engineering 2020.

Lee S., Dan N. T. 2005. Probabilistic landslide susceptibility mapping in the Lai Chau province of Vietnam: focus on the relationship between tectonic fractures and landslides. Environ Geol 48, 778-787.

Lee S., Park I., Choi J. K. 2012. Spatial Prediction of Ground Subsidence Susceptibility Using an Artificial Neural Network. Environmental Management 49: 347-358.

Lee s. and Park I. 2013. Application of decision tree model for the ground subsidence hazard mapping near abandoned underground coal mines. Journal of Environmental Management 127, 166-176.

Li Y., Lin Z., He L and Gong J. 2021. Effects of gradation and grain crushing on the liquefaction resistance of calcareous sand. Geomechanics and Geophysics for Geo-Energy and Geo-Resources 7, 12.

Lu C. C., Hwang J. H. and Hsu S. Y. 2017. The impact evaluation of soil liquefaction on low-rise building in the Meinong earthquake. Earth, Planets and Space 69, 109.

Maghsoudi Y., Amani R and Ahmadi H. 2021. A study of land subsidence in west of Tehran using Sentinel-1 data and permanent scatterer interferometric technique. Arabian Journal of Geosciences 14, 30.

Mohammady M., Pourghasemi H. R and Amiri M. 2019. Assessment of land subsidence susceptibility in Semnan plain (Iran): a comparison of support vector machine and weights of evidence data mining algorithms. Nat Hazards 99, 951-971.

Najafi Z., Pourghasemi H. R., Ghanbarian G., Shamsi S. R. F. 2020. Land-subsidence susceptibility zonation using remote sensing, GIS, and probability models in a Google Earth Engine platform. Environ Earth Sci 79, 491.

Nam K. and Wang F. 2019. The performance of using an autoencoder for prediction and susceptibility assessment of landslides: A case study on landslides triggered by the 2018 Hokkaido Eastern Iburi earthquake in Japan. Geoenviron Disasters 6, 19.

Oh H. J., Ahn S. C., Choi J. K., Lee. S. 2011. Sensitivity analysis for the GIS-based mapping of the ground subsidence hazard near abandoned underground coal mines. Environ Earth Sci 64, 347-358.

Oh H. J. and Lee. S. 2010. Assessment of ground subsidence using GIS and the weights-of-evidence model. Engineering Geology, 115(1-2), 36-48.

Oh H. J. and Lee. S. 2011. Integration of ground subsidence hazard maps of abandoned coal mines in Samcheok, Korea. International Journal of Coal Geology 86(1), 58-72.

Oh H. J., Syifa M., Lee C. W., Lee S. 2019. Land Subsidence Susceptibility Mapping Using Bayesian, Functional, and Meta-Ensemble Machine Learning Models. Applied Sciences, 9(6), 1248.

Park I. H., Lee J., Lee S. 2014. Ensemble of ground subsidence hazard maps using fuzzy logic. Central European Journal of Geosciences 6, 207-218.

Perrin J., Cartannaz C., Noury G., Vanoudheusden E. 2015. A multicriteria approach to karst subsidence hazard mapping supported by weights-of-evidence analysis. Engineering Geology 197, 296-305.

Pradhan B., Abokharima M. H., Jebur M. N., Tehrany M. S. 2014. Land subsidence susceptibility mapping at Kinta Valley (Malaysia) using the evidential belief function model in GIS. Nat Hazards 73, 1019-1042.

Rasyid A. R., Bhandary N. P., Yatabe R. 2016. Performance of frequency ratio and logistic regression model in creating GIS based landslides susceptibility map at Lompobattang Mountain, Indonesia. Geoenvironmental Disasters 3: 19.

Rehman S., Sahana M., Dutta S., Sajjad H., Song X., Imdad K., Dou J. 2020. Assessing subsidence susceptibility to coal mining using frequency ratio, statistical index and Mamdani fuzzy models: evidence from Raniganj coalfield, India. Environmental Earth Sciences 79: 380.

Sevil J., Gutiérrez F., Carnicer C., Carbonel D., Desir G., Arnay A., Guerrero J. 2020. Characterizing and monitoring a high-risk sinkhole in an urban areaunderlain by salt through non-invasive methods: Detailed mapping, high-precision leveling and GPR. Engineering Geology 272, 105641.

Singh K. B., Dhar B. B. 1997. Sinkhole subsidence due to mining. Geotech Geol Eng 15(4): 327-341

Ullah K., Zhang J., 2020. GIS-based flood hazard mapping using relative frequency ratio method: A case study of Panjkora River Basin, eastern Hindu Wardsh, Pakistan. PLOS ONE https://doi.org/10.1371/journal.pone.0229153.

USGS. Earthquakes. Retrieved from: https://earthquake.usgs.gov/earthquakes/search/

Waltham AC. 1989. Ground subsidence. Blackie, New York, p. 49-71.

Wang Z. L., Makdisi F. I., Egan J. 2006. Practical applications of a nonlinear approach to analysis of earthquake-induced liquefaction and deformation of earth structures. Soil Dynamics and Earthquake Engineering, 26(2-4), 231-252.

Yalcin A., Reis S., Aydinoglu A.C., Yomralioglu T. 2011. A GIS-based comparative study of frequency ratio, analytical hierarchy process, bivariate statistics and logistics regression methods for landslide susceptibility mapping in Trabzon, NE Turkey. CATENA 85(3), 274-287.

Yasuda S., Harada K., Ishikawa K., Kanemaru Y. 2012. Characteristics of liquefaction in Tokyo Bay area by the 2011 Great East Japan Earthquake. Soils and Foundations, Vol. 52(5), 793-810.

Zhou M., Wang F., Du Y. J. et al. 2019. Laboratory evaluation of buried high-density polyethylene pipes subjected to localized ground subsidence. Acta Geotech 14, 1081-1099.

Zhou H., Che A., Wang L & Wang L. 2021. Investigation and mechanism analysis of disasters under Hokkaido Eastern Iburi earthquake. Geomatics, Natural Hazards and Risk, 12(1), 1-28.